PL-TR-96-2227

OBSERVATION, ANALYSIS AND MODELING OF IONOSPHERIC TOTAL ELECTRON CONTENT (TEC) AND SCINTILLATION EFFECTS

C. Charley Andreasen
Edward J. Fremouw
Elizabeth Holland
Andrew Mazzella
G.-S. Rao
James A. Secan

NorthWest Research Associates, Inc.
14508 NE 20th Street
PO Box 3027
Bellevue, WA 98009-3027

1 July 1996

Scientific Report No. 2

Approved for public release; distribution unlimited

PHILLIPS LABORATORY
Directorate of Geophysics
AIR FORCE MATERIEL COMMAND
HANSCOM AFB, MA 01731-3010

"This technical report has been reviewed and is approved for publication"

GREGORY J. BISHOP
Contract Manager

DAVID N. ANDERSON
Branch Chief

DAVID A. HARDY
Division Director

This report has been reviewed by the ESC Public Affairs Office (PA) and is releasable to the National Technical Information Service (NTIS).

Qualified requestors may obtain additional copies from the Defense Technical Information Center (DTIC). All others should apply to the National Technical Information Service (NTIS).

If your address has changed, or if you wish to be removed from the mailing list, or if the addressee is no longer employed by your organization, please notify PL/IM, 29 Randolph Road, Hanscom AFB, MA 01731-3010. This will assist us in maintaining a current mailing list.

Do not return copies of this report unless contractual obligations or notices on a specific document requires that it be returned.

REPORT DOCUMENTATION PAGE

Form Approved
OMB No. 0704-0188

1. AGENCY USE ONLY *(Leave blank)*	2. REPORT DATE	3. REPORT TYPE AND DATES COVERED
	1 July 1996	Scientific No. 2

4. TITLE AND SUBTITLE
Observation, Analysis, and Modeling of Ionospheric Total Electron Content (TEC) and Scintillation Effects

5. FUNDING NUMBERS
F19628-94-C-0067
PE 62601F
PRDMSP
TASGH
WUAA

6. AUTHOR(S)
C. Charley Andreasen, Edward J. Fremouw, Elizabeth A. Holland, Andrew J. Mazzella, G.-S. Rao, James A. Secan

7. PERFORMING ORGANIZATION NAME(S) AND ADDRESS(ES)
Northwest Research Associates, Inc.
300 120th Ave NE, Bldg 7, Ste 220
P.O. Box 3027
Bellevue, WA 98009-3027

8. PERFORMING ORGANIZATION REPORT NUMBER
NWRA-CR-96-R157

9. SPONSORING / MONITORING AGENCY NAME(S) AND ADDRESS(ES)
Phillips Laboratory
29 Randolph Road
Hanscom AFB, MA 01731-3010
Contract Manager: Greg Bishop/GPIA

10. SPONSORING / MONITORING AGENCY REPORT NUMBER
PL-TR-96-2227

11. SUPPLEMENTARY NOTES
These studies will benefit the AF Space Forecast Center (50th Weather Squadron, AFPCS) by improving understanding of the behavior of ionospheric structure that can affect operations of various DOD customers.

12a. DISTRIBUTION / AVAILABILITY STATEMENT
Approved for public release; distribution unlimited

12b. DISTRIBUTION CODE

13. ABSTRACT (Maximum 200 words)

Many military systems used for communications, command and control, navigation, tracking, and surveillance depend on reliable and relatively noise-free transmission of radiowave signals through the earth's ionosphere. These systems can be affected by both large-scale features (> 1,000 km) and small-scale structures (< few hundred km) in the ionosphere, often leading to degraded operations. This report documents the results of the second year of a three-year investigation of various facets of this problem. Two study areas are reported on: (1) an investigation of methods for using signals from Global Positioning System (GPS) satellites to measure ionospheric Total Electron Content (TEC), including techniques for receiver calibrations, and (2) a study of the shape and behavior of the phase-scintillation power-density spectrum (PDS) over a scale-size range of 10s to 100s of kilometers. The TEC studies are still on-going; the phase PDS study found that the slope of the phase PDS at these scale sizes is steeper than those found in earlier studies at shorter scales.

14. SUBJECT TERMS
Ionosphere, Ionospheric density irregularities, Ionospheric Total Electron Content, Ionospheric modeling, Scintillation, Ionospheric measurements

15. NUMBER OF PAGES
64

16. PRICE CODE

17. SECURITY CLASSIFICATION OF REPORT	18. SECURITY CLASSIFICATION OF THIS PAGE	19. SECURITY CLASSIFICATION OF ABSTRACT	20. LIMITATION OF ABSTRACT
Unclassified	Unclassified	Unclassified	SAR

Contents Page

Figures

Tables

PREFACE

This report summarizes the work completed during the second year of a project focused on studies of the effects of the earth's ionosphere on transionospheric radiowave propagation.

We express our appreciation to SSgt. Carlton Curtis of Phillips Laboratory at Hanscom for his collaboration in many of the investigations and support efforts for the Ionospheric Measuring System and other TEC and scintillation measurement projects. We also express our appreciation to Peter Ning of KEO Consultants for his guidance and assistance in analyzing the visual all-sky images from the 1994 Chile campaign.

1. Introduction

The overall objective of the various tasks that make up this project is to improve our understanding of ionospheric effects on transionospheric radiowave propagation. The phenomena to be studied cover the full range of scale sizes from tens of meters (scintillation effects) to thousands of kilometers (large-scale TEC effects). The twelve tasks outlined in the proposal for this work [*Fremouw et al.*, 1994] can be grouped into the following six study areas. (The tasks in the proposal corresponding to these study areas are indicated in parentheses.)

1. Investigate the logarithmic slope of the phase-scintillation power-density spectrum (PDS) at large scales in the equatorial region. Develop a model for a two-regime power-law PDS based on the results of the investigation and implement it in WBMOD. (Tasks 1 and 2)

2. Investigate the magnitude and behavior of small-scale phase gradients using the equatorial scintillation data sets built in the first study. Develop algorithms for including the effects of small-scale phase gradients on transionospheric propagation based on the results of the investigation and implement them in the WBMOD ionospheric scintillation model. (Tasks 3 and 4)

3. Develop models consistent with the current propagation algorithm in WBMOD for individual intermediate-scale ionospheric features associated with enhanced scintillation (equatorial depletion plumes, polar patches, auroral boundary blobs). Implement these in WBMOD. (Tasks 5 and 6)

4. Develop techniques for producing short-term forecasts of scintillation effects over large spatial areas, implementing and demonstrating these techniques in computer programs. (Task 7)

5. Deploy, operate, and maintain satellite receiver instrumentation on a long-term basis at local and remote sites to collect databases of ionospheric Total Electron Content (TEC) and scintillation observations. Use these data to (a) analyze performance of ionospheric monitors, (b) validate models of ionospheric behavior, and (c) develop/formulate algorithms to improve the performance of both ionospheric monitors and models. (Tasks 8 and 9)

6. Deploy, operate, and maintain satellite receiver instrumentation on a short-term basis at local and remote sites where unique opportunities exist for enhancement of test data sets, particularly where other instruments have been deployed to collect other ionospheric measurements. Collect these data, and ancillary data from other instrumentation, into documented data sets that can be used as outlined in the previous study description. (Tasks 8, 9, and 12)

[Note: Task 11 is not explicitly included in the above listing as it includes support to all of the various tasks described in the proposal.]

2. Ionospheric Total Electron Content Studies

Investigations of ionospheric Total Electron Content (TEC) are being performed based on current data acquired from the Air Force Ionospheric Measuring System (IMS) stations being deployed globally, as well as other measurement systems deployed on a temporary or permanent basis. Previously acquired data are also being processed and analyzed to investigate ionospheric conditions at alternative times and locations. All of these systems utilize single-frequency or dual-frequency GPS receivers.

The sources of ionospheric-measurement data utilized during this period of study encompass the following:

1. IMS stations deployed at Otis Air National Guard Base, Massachusetts; Croughton Royal Air Force Base, England; Thule Air Base, Greenland;

2. An IMS operating at Phillips Laboratory at Hanscom, Massachusetts, for check-out, diagnostic, and developmental efforts, prior to its shipment to Eareckson Air Force Station, Shemya, Alaska;

3. Data sets recorded at Shemya, Alaska, by the Real-Time Monitor developed by the University of Texas Applied Research Laboratory, in support of the site survey for installation of the IMS at that site;

4. A portable single-frequency GPS receiver deployed for an ionospheric study campaign at Agua Verde, Chile, in September and October of 1994;

5. Data available on electronic networks from GPS maintenance and research centers.

2.1 General Analysis. Assistance was provided to personnel of Phillips Laboratory at Hanscom (PLH) in installing and configuring software on a notebook PC to allow data collection and near-real-time display of scintillation and TEC, as reported by a single-frequency GPS receiver. This system was deployed on relatively short notice for a special campaign in Italy. Further GPS data-processing procedures and programs were installed on another notebook PC for use with data collected by a stand-alone Ashtech receiver and antenna system. This notebook system is also being deployed for field work on an interim basis, was used during this period to evaluate data collected for comparison to the IMS operating at PLH, Thule, and Otis, and was deployed for use during the site survey at Shemya.

Ionospheric measurements were acquired from the National Oceanic and Atmospheric Administration's (NOAA) Continuously Operating Reference Station (CORS) network, which is managed by the National Geodetic Survey (NGS), for their station at Portsmouth, New Hampshire. Although the initial data-acquisition processing was different for these data sets, many of the processing steps were common with prior processing for data in RINEX format, and two days of data (95-169, 95-174) were evaluated for satellite and receiver biases. A bias shift of about 9 TEC units is evident between the two days, which is compatible with the reported change in receivers.

Procedures have been developed to utilize the standard Windows-NT FTP utility to retrieve TEC data files from either the NOAA CORS network, or the Jet Propulsion Laboratory (JPL)

distribution center. Additional procedures were developed to convert these files into a standard format suitable for display and analysis.

The dialup process of obtaining GPS almanac files from Holloman AFB, New Mexico, was almost totally automated, and now requires only a simple manual initiation to update the existing archive of almanac files. Almanac files are retrieved as needed for calibration calculations and other GPS ephemeris studies.

Two programs were developed to address data anomalies that can severely affect the bias determinations for dual-frequency GPS systems, reducing the need for manual review and editing of the data or even possible elimination of some data segments. The first program was developed to address the problem of discontinuities in the Differential Carrier Phase (DCP) during a satellite pass, generally caused by a loss of lock in tracking the satellite. The amplitude of the phase discontinuity is estimated from the DCP profile on either side of the discontinuity, and the subsequent portion of the DCP profile is adjusted by this amount to produce a more smoothly varying slant TEC profile. This editing step precedes the phase-averaging process used to align the DCP with the Differential Group Delay (DGD), and enhances that process by allowing averaging over a longer time interval. The second program was developed to eliminate unreasonable DGD values, which generally occur when a satellite is first acquired for tracking or at low elevations. This step also enhances the phase-averaging process, because extreme DGD outliers can seriously degrade the accuracy for phase-averaging. Additional enhancements were incorporated into data-processing programs for bias calculations, to estimate the error arising from phase-averaging.

An investigation was conducted into the effects of utilizing an elevation-dependent weighting function for phase-averaging, to alleviate the influence of noise in the DGD signal at low elevations. In conjunction with this study, the plotting program used to display the differential group and phase data was extended to allow these quantities to be overplotted on the same frame. Further effort is required to pursue this investigation.

The bias-calculation method was examined for effects of decimating data, to evaluate the computational speed advantages against the potential loss of accuracy. A significant computational time reduction was obtained with relatively minor bias errors (less than 0.5 TEC units) up to a decimation factor of 40, corresponding to one data sample every 20 minutes. The computational time required at this level of decimation was less than one minute, on a 90 MHz Pentium. Results of this investigation are displayed in Figure 1.

The sensitivity of the bias-calculation method to the absence of one or more satellites from the data-collection set was also investigated. Using bias values determined from a full complement of 25 GPS satellites as a reference, comparative bias values were calculated for the successive elimination of individual satellites, up to a total of eight satellites. For the particular sequence of eliminations used, the maximum error in the calculated biases was only one TEC unit. These results have applicability to the comparison of measurements performed at different GPS receiver sites, where the satellite coverage varies.

A

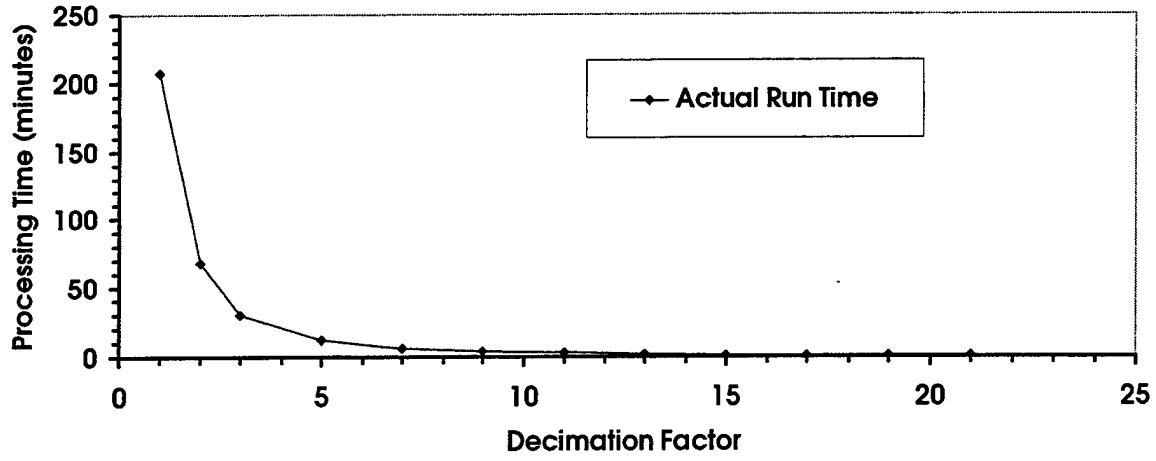

B

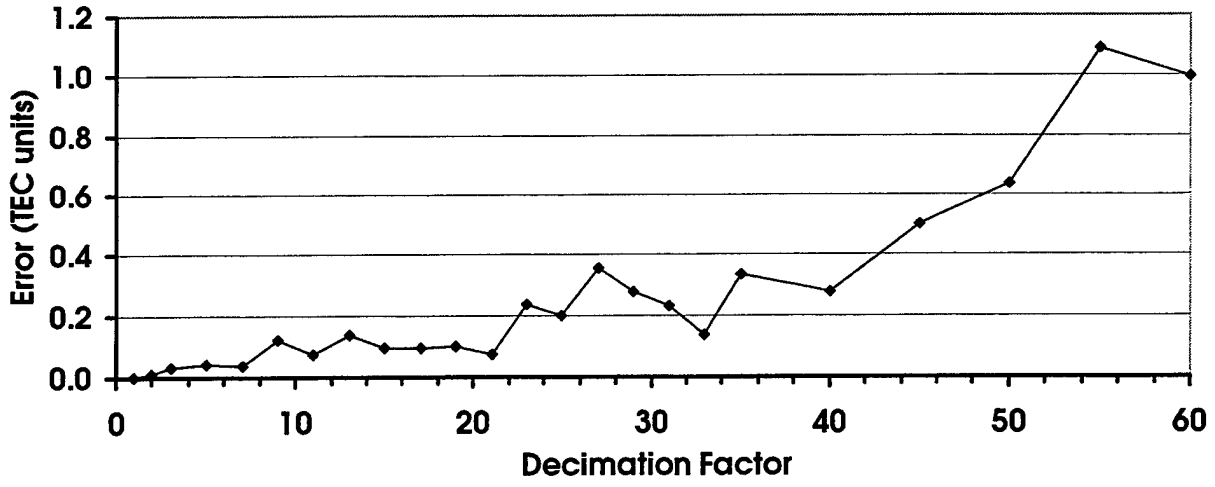

Figure 1. A. Processing time for bias calculations with varying degrees of data decimation. B. Maximum bias error, in TEC units, for bias calculation with varying degrees of data decimation.

The applicability of the bias determination to short time intervals was investigated by performing the bias calculations for six-hour intervals at seven overlapping periods within a day, for each of six days. The multipath error effect for phase-averaging was minimized for these tests by performing phase-averaging over complete passes, but significant bias errors were still observable for passes that were only marginally included in the six-hour intervals. Restricting the calculation to passes that substantially overlapped the interval produced improvement, but still generated distinct differences in the vertical TEC profile and in the estimated receiver biases of up to four TEC units.

The detectability of errors in the bias determinations was investigated by introducing artificial shifts in the bias values and examining the resulting diurnal vertical TEC profiles. A marginal decrease in the self-consistency of the diurnal profile is evident for a bias shift of one TEC unit, and a generally perceptible decrease in the self-consistency of the diurnal profile is evident for a bias shift of three TEC units.

The standard plotting program for displaying diurnal vertical TEC profiles was enhanced to allow Universal Time (UT) to be used as the independent variable, instead of the local time at the Ionospheric Penetration Point (IPP). This plotting enhancement allows the satellite coverage to be displayed in terms of the actual data-acquisition time.

Previous calibration of data from 94-114 collected by PLH on-site at Hanscom AFB, MA, and by the Jet Propulsion Laboratory at Westford, MA, yielded diurnal TEC variations that diverged over the latter half of the day. These data were reviewed to determine the cause of the discrepancy. Each satellite pass in both data sets was examined for characteristics that adversely affect quality, such as large multipath content and discontinuities, which cause the differential phase reference level from phase-averaging to be incorrect. Short passes of less than ninety minutes also yield incorrect reference levels when phase-averaged. The Westford differential group delays were found to contain some very large multipath associated with data from elevations below twenty degrees, so each pass was edited to remove low elevation, high multipath sections. The Hanscom data were edited to remove high multipath sections. Passes containing discontinuities were segmented into separate files, with pass segments less than ninety minutes duration being deleted from either data set. Recalibration of the edited data sets produced diurnal curves that are much less divergent overall. For the original calibration, the curves are divergent from 0600 to 2000 IPP local time, and the maximum discrepancy is three TEC units. The calibration of the edited files resulted in curves that agree to within one TEC unit for most of the day, with a maximum discrepancy of less than two TEC units in the 1600 to 2000 IPP local time period. These results indicate that the disagreement in the diurnal curves from the initial calibration is the result of low elevation, high multipath, discontinuous, or short data segments.

Data previously recorded using the Real-Time Monitor (RTM) system obtained from Applied Research Laboratories (ARL) at the University of Texas at Austin were reviewed, to evaluate a problem in continuously tracking GPS satellites. The recorded values indicate that some satellites are observed throughout their period of visibility, but that a loss of lock for the phase occurs for most of that time. This problem has occurred for the RTM system during its deployment at Shemya, Thule, and Otis, but appears to have been minimal for its deployment at Croughton. Recommendations were obtained from ARL personnel for techniques in further diagnosing this problem, and new data were recorded. An additional reference file was generated in conjunction with one of these data sets, to report more details of the actual receiver data and not just results from the data-collection program. These results were discussed with personnel from ARL, and data files were transferred to them for further analysis. Their observation was that, when the loss of lock in satellite tracking occurred, it apparently occurred only in the L2 frequency. Evaluation of this situation is continuing.

Procedures were developed in Interactive Data Language (IDL) for the display of TEC maps based on data from one GPS receiver station. The display options included a three-dimensional mesh representation and a color contour representation of equivalent vertical TEC versus latitude

and local time, and a color contour representation of equivalent vertical TEC on a global map. A three-dimensional mesh representation for equivalent vertical TEC for day 94-119 at ARL is displayed in Figure 2. These are the same data that were displayed as latitude bands in Figure 1 in "Analysis of Ionospheric Monitoring System (IMS) Total Electron Content (TEC) Data and Equatorial Phase-Scintillation Data" [*Secan et al.*, 1995].

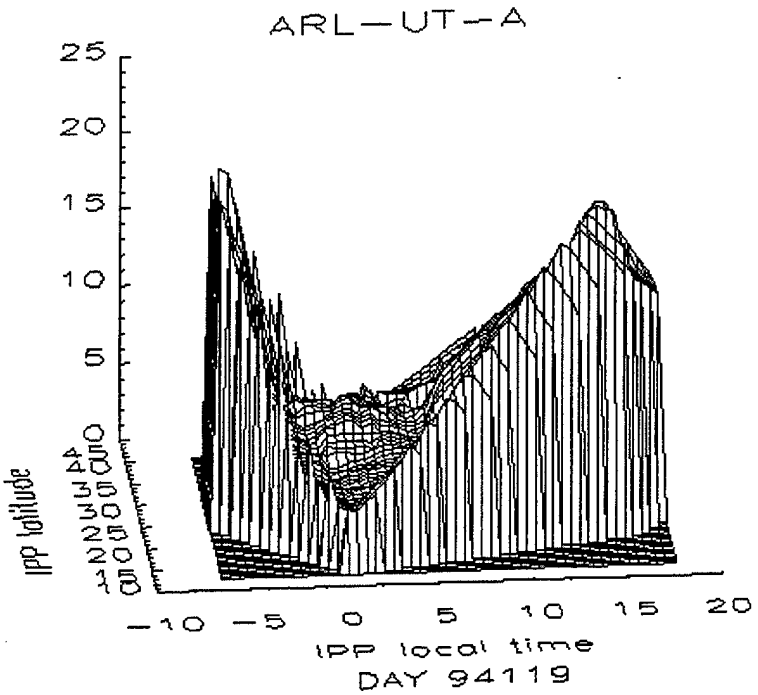

Figure 2. Three-dimensional mesh representation for equivalent vertical TEC versus latitude and local time at the Ionospheric Penetration Point (IPP), for day 119 of 1994 (29 Apr 1994).

2.2 Ionospheric Measuring System

2.2.1 IMS Companion PCs. A set of Pentium PC systems has been configured for each currently scheduled IMS deployment, for data-acquisition support and on-site processing. Enhanced communications capabilities and recent software improvements have resolved the earlier data-acquisition problems, and permitted the offloading of some data-processing stages onto the deployed PC. In particular, the One-Minute data extraction from the IMS archive files now occurs in near-real-time as these files are transferred from the IMS. An automated tape-archiving process was also implemented on the PC. The basic roles of the IMS and its companion PC are displayed in Table 1.

Table 1. Basic functions performed by the IMS and their companion PCs.

IMS Function	Companion PC
Data collection	High-speed dialup connection
Data validation	Data archiving
Vertical TEC calculation	Data tabulation for display
TELSI transmission	Calibration support

The Otis PC experienced a hard-disk failure in early December 1995, and was replaced during a planned visit to Otis, utilizing another Pentium PC that had been configured for deployment with the Shemya IMS. Consequently, a new Pentium PC was configured as a replacement for deployment with the Shemya IMS. A similar Pentium PC that had been configured for use both at remote IMS sites and locally as a data-acquisition and remote-monitoring system had also experienced a hard-disk failure in early November 1995. This disk was replaced without difficulty, but the warranty period had expired by the time of the Otis PC disk failure, so a disk exchange was required. The situation has been discussed between PLH personnel and the disk manufacturer, and there is a likelihood that both disks could have been from a single batch that had defects.

During the latter part of February 1996, the Pentium PC system that was deployed with the Croughton IMS for data-acquisition support and on-site processing experienced a number of intermittent interruptions during remote operating sessions and was frequently unresponsive to remote session initiation without a full power reset. To alleviate this problem, and at the same time achieve a major system and processing software upgrade, the Pentium PC that had been retrieved from Otis in December 1995 was refurbished with a new hard disk, loaded with the most recent software, tested, and shipped to Croughton RAF, UK, as a replacement. The former Croughton PC was then shipped back to PLH for examination and testing. An initial examination of this PC by PLH and NWRA personnel revealed a failure of the processor chip cooling fan, which was replaced, and some difficulties with the network board, which was also replaced. The hard disk was also closely examined, given the previous experience with similar disks obtained at that time. The replacement PC has performed well at Croughton since its installation, although sporadic communications problems are still encountered.

During the early part of March 1996, the Pentium PC system that was deployed with the Thule IMS for data-acquisition support and on-site processing was recognized as requiring a significant software upgrade, particularly with regard to preliminary software versions implemented with an expiration date. To address this situation, the Pentium PC that had been shipped from Croughton RAF, UK, in February 1996 and refurbished, was loaded with the most recent software, tested, and shipped to Thule Air Base, Greenland, in mid-April 1996 as a replacement. The original Thule companion PC was left at the site until the maintenance visit to Thule in late June 1996.

The local PC used to monitor the remote IMS sites experienced a brief interruption in service when the fan for the power supply failed, causing an overheating problem. A temporary remedy was implemented until a new power supply was received and installed.

A development plan has been formulated to implement autonomous bias calibrations at the individual IMS sites, utilizing TEC data acquired from each IMS by its companion PC on a near-real-time basis. Issues addressed by the plan include data-quality checking, phase-discontinuity correction, reliable phase-averaging calculations, improved bias calculations, and implementation of the bias corrections on the IMS. A phased implementation is planned, both to monitor the effects of automating each step and to reduce the manual workload required in monitoring each site at the earliest opportunities.

To expedite on-line data acquisition at PLH from the remote PC at each IMS site, a new procedure was developed and tested to automate the initial stages of the IMS data extraction and reformatting. This new procedure allows the number of telephone connections to each PC to be reduced. The same procedure was uploaded to the companion PCs at Thule, Croughton, and Otis, and was installed on the companion PC for Shemya before shipping.

On-site, autonomous processing capabilities for the companion PC at each IMS site were augmented by development of a daily process to concatenate the 15-minute duration pass file segments that are generated in near-real-time in association with the data-transfer process from the IMS. A further maintenance automation was achieved by the development of a process to delete intermediate data files more than three days old. This process can also be utilized to delete IMS archive files that have been written to the PC backup tape.

The program that performs the concatenation of the 15-minute pass file segments was enhanced to allow more flexibility in setting segmenting thresholds and to improve the criteria used in the concatenation process.

2.2.2 IMS Procedures. The UNIX scripts that were previously developed for data-file transfers from the IMS to its companion PC were adapted for installation on the Thule IMS, which was deployed at Thule Air Base, Greenland, during the latter part of August 1995. Some of the revisions were required for site-specific addressing conventions, while most of the others were implemented to interact properly with the different network program being utilized on that and subsequently deployed PCs. Provisions for real-time data transfer were incorporated into the new procedures, and these have worked well with the new PC FTP server. These UNIX scripts have also been augmented to require less operator intervention for initialization and error conditions, and to provide more diagnostic logging information.

To reduce operator maintenance efforts for the remote IMS sites, a new procedure was developed, tested, and uploaded to the Otis IMS, Croughton IMS, and Thule IMS to delete data files older than a specified number of days (typically five) from the intermediate data-archiving directory allocated to operational maintenance. These files were originally maintained as part of the stopgap procedure developed to overcome the problems with the original IMS tape archiving, and are currently maintained only as a backup to the near-real-time data transfer to the companion PC at each site.

Coordinated investigations were conducted with personnel from the Charles Stark Draper Laboratory (CSDL) to investigate the source of very large DGD values during the initial minutes of a satellite pass. Data segments exhibiting such features in the 1-minute or 15-minute sample averages were re-examined at the original 2-Hz data-sampling rate, including the data quality and warning flags and signal strength as well as the measured DGD and DCP. It was found that non-zero warning flags were associated with extreme and irregular variations in DGD, so CSDL

personnel implemented a change in the initial data collection and processing stages to check the appropriate flags before utilizing the data for the time-averaging. A secondary elevation threshold was also instituted, so that data samples below this elevation would be excluded from the time-averaging. Both of these changes were tested on the IMS at PLH, and were installed on the IMS at Otis, Croughton, and Thule when satisfactory test results were achieved.

2.2.3 Ghost Satellites. Further investigations into the IMS "ghost" satellites (GPS satellites that are spuriously reported by the IMS) have been conducted. These investigations included the examination of data stored by a stand-alone receiver of the same type as used in the IMS, a time-occurrence survey for "ghost" occurrences on the Otis IMS, a survey of "ghost" occurrences for the Croughton IMS, and "ghost" occurrences associated with different antennas.

Data collected at PLH using both a stand-alone receiver and the IMS yielded no ghosts, but in neither case was an IMS antenna assembly utilized, because no operational spare assemblies were available locally. A new Ashtech receiver was installed for the Otis IMS in early November 1995, but examination of the collected data still showed the presence of ghosts. An effort was coordinated with CSDL and PLH personnel to evaluate data captured directly from the Otis IMS receiver, bypassing the normal IMS processing, and joint analysis of this period demonstrated the occurrence of ghosts in the receiver data concurrent with those appearing in the normal IMS processing. The procedures for acquiring and evaluating GPS ephemeris data reported by the IMS were considerably enhanced and streamlined in order to pursue this investigation, because the ephemeris data have proven to be the best indicator of ghosts.

The RTM notebook PC configured for GPS data collection was temporarily installed at Otis ANGB with its own receiver and antenna, in the same vicinity as the IMS at that site. During the first day of data collection, the RTM system detected no ghosts, while the IMS continued detecting ghosts. The antennas for the IMS and the RTM system were exchanged for the second day of data collection, and no ghosts were detected by the IMS for that configuration, while the RTM system did detect ghosts. These results indicated that the ghost problem was not associated with the site environment, but was strongly linked to the antenna.

An Ashtech antenna was installed at Otis on the roof of the building containing the IMS, and was connected to the IMS by an alternative cabling system. Concurrently, a process was developed to expedite review of the GPS ephemeris information reported by the IMS, to enable the detection of "ghost" GPS satellites. This system configuration was examined for "ghosts" for over a month without any observed occurrences, except on one day when the data appear to have been contaminated by reports from the previous antenna.

Difficulty in maintaining a stable calibration for the Otis IMS after the installation of the roof Ashtech antenna led to a detailed investigation of the data being recorded by the IMS. It was determined that the DGD signals reported in the One-Minute data were highly variable from day to day, in a manner inconsistent with the degree of multipath variation normally observed. A number of diagnostic evaluations were conducted by PLH personnel, including changing the antenna, performing an RF spectral examination, and shortening the antenna cable, but none of these resolved the problem. Finally, NWRA and PLH personnel installed an Ashtech antenna in the IMS antenna housing, at a considerable distance from the IMS building, and the problem appears to have been circumvented, together with the elimination of ghosts.

Two further experiments were performed for investigating the problem of "ghosts". The original IMS Micropulse antenna that was shipped to CSDL with the fifth IMS was installed at PLH in early February 1996, and was found to produce "ghosts" within its first two days of operation. This antenna was installed without its accompanying housing. An Ashtech antenna was then installed in the IMS antenna housing in early March 1996, at a comparable location at PLH, and was examined using the same procedures earlier employed for Otis, without the detection of any "ghosts" for a period of three weeks.

2.2.4 Operations. Data files continue to be processed, reviewed, and archived to tape at each of the deployed IMS sites at Thule, Greenland; Croughton, United Kingdom; and Otis ANGB, Massachusetts; with the archive tapes being shipped to PLH for cataloguing. The development, testing, and data-archiving operations of the PLH IMS and its companion Pentium PC were discontinued in mid-June 1996, with the shipment of those systems to Eareckson AFS, Alaska. The data-transfer process from the IMS to its companion PC at all deployed sites has been improved to ensure that all data files generated by the IMS are eventually transferred to the PC, even if the PC FTP server is not active at the originally scheduled transfer time.

A summary log is being maintained for the IMS at Otis, the IMS at Croughton, and the IMS at Thule, primarily to monitor the duration of operations for each of the two UNIX computer systems in each IMS. The cause of the system shutdown is also recorded in this log. A script has been developed to process the status-report files from the IMS and automatically update this summary log. Utilization of this script, in conjunction with a processor-identification report to the on-site system log, has greatly facilitated this log maintenance.

Otis. The IMS at Otis had been experiencing a sporadic problem in initializing one of its pair of processors, but finally encountered a situation in late January 1996 where neither processor could be initialized, disabling the entire system. Based on similar symptoms encountered with other IMS processors prior to their SCSI cabling reconfiguration, the IMS failure at Otis was diagnosed as a late appearance of this same cabling problem, because the Otis IMS has not yet been cabled in the revised configuration. Rather than implement a full cabling reconfiguration, however, with the associated disassembly and reassembly of the entire equipment rack, only a partial cabling reconfiguration was performed, with the insertion of an electronic SCSI cable terminator. The Otis IMS was then restored to operational status.

Croughton. The IMS at Croughton RAF Base in England was operational until 20 July 1995, by which time both the direct dialup connection and the companion PC for that site were not operational. The direct dialup connections were restored on 6 September 1995, and one of the new Pentium PC systems was delivered as a replacement for the original PC. On-line data file-storage procedures were temporarily circumvented on the IMS, to attain minimal operational status of the IMS. The original PC has been returned to PLH for diagnosis and possible reconfiguration as a spare. Local support at PLH was provided to PLH personnel working at Croughton during the re-installation of the Netblazer, installation of the new PC, and loading and configuration of the new software on the IMS there.

The IMS at Croughton RAF Base in England was then operating in a stand-alone mode until 15 November 1995, although it was accessible by direct dialup connection and through its companion PC. However, it was not issuing data reports to its network connection. On 15 November 1995, a joint effort with PLH personnel diagnosed and corrected a serial port

parameter setting, and data reports began to appear at 50th Weather Squadron (50WS) from the Croughton IMS. Unfortunately, the stability of the IMS was adversely affected by the additional communications activity, and system shutdowns became quite frequent (up to 44 per day). Consequently, the data are too severely fragmented to process without extensive effort.

To assist with the CSDL analysis of the frequent system shutdowns of the Croughton IMS, a Full Debug mode was initiated on the Croughton IMS by NWRA in January 1996, and the resulting log files were retrieved after a week of operation in this mode. These files were downloaded from the Croughton IMS through the Croughton companion PC, and were made available to CSDL on the NWRA FTP server system.

The operational problems for the Croughton IMS were substantially resolved by the CSDL personnel by 29 February 1996, so the Croughton IMS is now regularly transmitting TEC reports (TELSI messages) to 50WS, the Croughton PC is now regularly receiving data files from the IMS, and the software update associated with the PC exchange in March 1996 has expanded the near-real-time and automated data management and processing capabilities.

A maintenance visit to Croughton RAF was performed in early May 1996 to change the GPS antenna for the IMS there for alleviation of the "ghost" problem, install an RF filter for the GPS receiver, install new clock batteries and UPS batteries, and perform general system maintenance. An initial calibration was performed remotely to compensate for the antenna and RF filter installation, and was implemented as just a change in the receiver bias value. A subsequent calibration, using a complete day of data, was performed to adjust both the satellite and receiver bias values.

Initial examination of the 15-Minute TEC data from the Croughton IMS in the period following the antenna change and associated bias calibration indicated that another calibration was soon required, but processing of the One-Minute data to derive a calibration showed much better agreement with the existing calibration. A detailed examination of the One-Minute data, and, in some cases, its underlying 2-Hz data, validated the stability in the DGD multipath, unlike an earlier situation for the IMS at Otis. However, the multipath amplitude appeared to have increased with the change of the antenna, and this increase also accentuated a provision in the initial data processing in which a small set of 2-Hz data samples constitute a full One-Minute sample, resulting in a "wild point" at the beginning or end of a satellite pass.

A further evaluation of the multipath effect on the 15-Minute TEC data reports from the Croughton IMS was conducted, by calculating the cumulative phase-averaging as the satellite pass progressed, rather than only at the end of the satellite pass. Because of the long-period multipath, the cumulative phase-averaging adjustment approaches its final value only asymptotically, and can differ from this value by 2 to 5 TEC units over much of the satellite pass. This difference then appears as a bias error for most of the 15-minute TEC reports, mimicking a poor calibration.

Thule. Data accumulated at PLH in June and July 1995 during the testing phase for the IMS to be deployed at Thule Air Base, Greenland, were archived to tape for future analysis.

On-site support was provided for the Thule IMS installation, spanning the period 14 August 1995 to 26 August 1995. This effort included proper configuration of the IMS rack, diagnosis

for a faulty antenna for GPS signals, and general performance validation and optimization. This effort was successfully concluded after the preliminary evaluation of the data at PLH.

To corroborate the Thule IMS data, a data set collected by the installation team using the RTM system was also processed. Despite being only a partial day and commencing just prior to the IMS operation, an encouraging general consistency was obtained.

The IMS at Thule was operating originally in a stand-alone mode, with no data reports, but with dialup connections and communication with its companion PC. In preparation for network operations, the revised IMS software that was delivered to PLH in September 1995 was installed on both processors of the Thule IMS. Portions of this software package were superseded by software installed during the June 1996 maintenance visit.

A maintenance visit to Thule Air Base was performed in mid-June 1996 to change the GPS antenna for the IMS there for alleviation of the "ghost" problem, install new clock batteries, deliver new UPS batteries, and perform general system maintenance. A thorough investigation was conducted of the continued failure to receive TELSI transmissions from the Thule IMS, including serial port parameter settings, communications links, and telephone line quality. This problem was successfully resolved, and TELSI transmissions have since been received regularly by 50WS.

During the latter portion of the Thule maintenance visit, a significant problem of temperature variations in the building containing the IMS was addressed. The building was found to become excessively warm during the Arctic 24-hour daylight, so the transfer and installation of fans and vents from another building were arranged. During this installation period, the IMS experienced low-temperature shutdowns due to a snowstorm, requiring telephone contacts with local technicians to restart the system.

Hanscom/Shemya. Data accumulated at PLH during the testing phase for the IMS to be deployed at Shemya, Alaska, were processed, reviewed, and archived to tape for future analysis. This IMS and its companion Pentium PC were also utilized for procedural-improvement testing, data quality and diagnostic investigations, and software testing.

After several months of use for configuration testing, development, and diagnostic investigations, the hard drive for the companion PC at PLH experienced a severe deterioration, and was replaced. The PC system was then reconfigured in its original role as the companion PC for the Shemya IMS, and underwent further testing for about a month before being shipped for deployment. This was the fourth original hard drive of this group of six PCs to fail. Replacement hard drives have been obtained from the vendor in all cases.

A site survey was conducted at Eareckson AFS, Shemya, Alaska, in preparation for the IMS to be installed there. Unfortunately, the RTM computer shipped for data collection and processing for the survey was offloaded at the wrong site, and was unavailable for the entire planned duration of the visit. A computer at the site, which had previously been utilized for the Real-Time Monitor and Scale Factor Generation support, was reconfigured for data collection using the new receiver and antenna shipped for the site survey, utilizing software uploaded by telephone from PLH. Operation of this system was monitored both on-site and remotely for the first two days, after which an RF filter was installed and a short period of on-site monitoring ensued. Following the site visit, remote monitoring was invoked, to retrieve a total of 19 days of

data, of which nine days were processed and six days extensively examined. Some interference at the GPS antenna was observed, but this does not appear to be associated with the radar at the site. A more detailed discussion of the site survey results is given in Appendix A.

CSDL. The fifth IMS, designated for deployment at Diego Garcia, was returned to CSDL from SM-ALC at McClellan Air Force Base, Sacramento, California, and was reassembled in early February 1996 with assistance from NWRA personnel. A pair of personal computers was also configured to accompany the IMS at CSDL, in "site companion" and "remote dialup" roles, analogous to the network operated from PLH. The remote dialup PC at CSDL and the companion PC at Croughton proved to be essential to CSDL in installing their repaired software on the Croughton IMS in late February 1996.

Data from the fifth IMS, taken during its period of operation in Sacramento, were examined for a potential problem of dual occurrences of a single GPS satellite on different receiver channels. This situation was found only to occur when two distinct satellite passes occurred during the day, and receiver channel switching during a pass did not occur for the recorded data.

2.2.5 Software. As a supplementary study for the DGD variability observed during antenna tests at Otis, a process was developed to examine the signal to noise ratio at the two receiver frequencies for each satellite being observed. This process was applied to the IMS at Otis and, for reference, the IMS at PLH, which was also using an Ashtech antenna at that time. The signal patterns were quite similar for the two Ashtech antennas, but distinctly different from the pattern for the Micropulse antenna that had formerly been installed at Otis.

Several programs were modified to incorporate the satellite and receiver biases removed by the IMS pre-processing stages back into the One-Minute slant TEC measurements, to allow for consistency in the slant TEC measurements across calibration updates. The resulting biases are then calculated on an absolute, rather than relative, baseline, and the calibration value conversions for the IMS are somewhat simplified.

An additional plotting program has been developed to display the 15-minute interval values for mean vertical TEC, maximum vertical TEC, and minimum vertical TEC, as extracted from the IMS data-archive files. These values are equivalent to those reported to 50WS as TELSI messages, and can be directly used to monitor the data quality of those messages. Similar displays had previously been generated using a spreadsheet program, with much time-consuming preparation and formatting. However, the original display technique did allow the demonstration of a simple criterion for eliminating wild TEC samples.

This plotting program for displaying the 15-minute interval values was extended to allow selection of latitude and longitude ranges. With these enhancements, the displayed diurnal profiles for equivalent vertical TEC can be used to evaluate the accuracy of the calibration being utilized within the IMS. Procedures have been developed to utilize this plotting program in this manner, greatly facilitating the evaluation of the calibration accuracy and the assessment of the need for re-calibration. A variation of this plotting program was developed to allow the display of IMS TELSI transmission data from the database maintained by 50WS. This allows for their review of data in a format comparable to that used at PLH with the NWRA software. A further revision of this program was incorporated to assign the contiguous longitude domain (-180 degrees to 180 degrees or 0 degrees to 360 degrees) more appropriately when mapping

measurements to local time at the Ionospheric Penetration Point. This produces a more accurate representation of the diurnal TEC profile.

2.2.6 Calibrations. Data files were retrieved as needed from the individual IMS sites and were used to evaluate the performance of the current bias definitions for the IMS and to calculate corrections and revised bias values for installation on the IMS. These data have also been reviewed for anomalous and spurious TEC measurements, as part of the continued assessment of the IMS performance. The days of data retrieved for bias calibrations at the deployed sites are listed in Table 2.

An evaluation for the Otis IMS utilizing data for 11 September 1995 revealed a sudden change in the DGD values of about 6 TEC units, for all satellites being observed at 5:50 Universal Time. This necessitated a bias correction, but also illustrated a potential problem in maintaining the calibration of the IMS, in that a sudden condition, in addition to the expected slow receiver bias drift, must be accommodated.

Table 2. Dates of data utilized for receiver and satellites bias calibrations.

Otis	Croughton	Thule
17 July 1995	19 March 1996	24 August 1995
27 August 1995	*19 May 1996	21 April 1996
12 September 1995		*20 June 1996
15 October 1995		
23 October 1995		
29 October 1995		
14 November 1995		
*12 December 1995		
15 January 1996		
*24 January 1996		
8 February 1996		
12 February 1996		
23 March 1996		
10 June 1996		

*These calibrations were required by an antenna change.

2.3 Single-Frequency Ionospheric Measurements. The Differential Carrier Phase and Differential Group Delay data from 1994 PLH GPS measurements were used in a simulation of single-frequency bias determination. The slant TEC from Differential Carrier Phase, which is only a measure of relative slant TEC, was input to the single-frequency calibration process. The resulting diurnal profile for equivalent vertical TEC was generally within two TEC units of that derived from phase-averaged data, which utilizes the absolute Differential Group Delay as a reference, but diverged to about five TEC units toward the end of the day. A similar experiment was performed using slant TEC from Differential Group Delay, which is significantly contaminated by noise and multipath, and therefore more closely simulates the single-frequency data in this regard. These data were smoothed using a sliding average process to decrease noise and multipath and were then input to the calibration process for single-frequency data, as individual satellite passes. Despite a resultant noise level of about one TEC unit, quantitative agreement with the dual-frequency TEC calculation was achieved to within approximately three TEC units, with a peak diurnal TEC amplitude of only about 15 TEC units. A number of enhancements in smoothing the slant TEC data were implemented as part of this investigation.

Data collected with the Trimble Pathfinder single-frequency GPS receiver were also used to study the adaptation of the bias-determination process for use with single-frequency GPS measurements. The single-frequency results were compared to slant TEC calculated from dual-frequency differential data, and the values were found to diverge in some cases. Analysis of this problem was pursued, addressing round-off errors for the time tag, pseudo-range, and Doppler values, but the discrepancy was not resolved in this initial investigation. Diurnal profiles calculated using this data set produced only rough agreement with the dual-frequency results, even with significant smoothing of the slant TEC.

These Trimble Pathfinder data sets were subsequently re-examined in an attempt to improve the calculation for slant TEC from pseudo-range and Doppler measurements, thus allowing the possibility of calibration for equivalent vertical TEC using the current methods. Direct comparison of slant TEC calculated for the Pathfinder data collected at PLH to dual-frequency slant TEC collected by the IMS at Otis repeatedly showed a divergence with time, even though both systems are viewing essentially the same ionospheric region. The nature of the divergence indicated a possible time difference between the pseudo-range and Doppler data samples for the Pathfinder, and, experimentally, a time difference of 0.004 seconds was observed to bring many of the Pathfinder and IMS satellite passes into agreement, although significant discrepancies remained for other passes, of the same divergent nature as previously. A calibration of the resulting single-frequency slant TEC data produced a diurnal ionospheric TEC profile that differed by about eight TEC units from that derived from the IMS data.

Single-frequency GPS data collected during the Chile campaign of 1994 were reviewed, in connection with visual all-sky images also produced from that campaign. With the assistance of personnel from KEO Consultants, apparent GPS satellite positions during periods of scintillation, as determined by the single-frequency amplitude variations, were coordinated with dark regions of 630.0 nm airglow, which are associated with TEC depletions. Charts of the observing geometry were constructed for a number of instances in the course of the observations, displaying the vertical propagation of disturbances in the airglow layer and the ionosphere, as well as the lines-of-sight from the observing station to the GPS satellites [*Bishop et al.*, 1996]. An item that was investigated further was a small error in the calculated azimuths and elevations for GPS

satellites at the Agua Verde, Chile, site, as compared to calculations from an independent source. The discrepancy was ultimately traced to an error in the units used for the site altitude. In the course of this investigation, the programs used for the calculations were enhanced for greater versatility in handling date ranges and year-to-year transitions, and in preserving the numerical precision of the acquired data values.

Single-frequency GPS data collected at PLH as test data for the forthcoming fall Chile campaign were reviewed, to evaluate the resolution available for the signal strength parameter. The data appeared comparable to those previously obtained by the single-frequency Trimble Pathfinder receiver, which has been successfully deployed for measurement of scintillation occurrences, so further utilization of data from this new receiver is planned. This is a significant extension of the role of this receiver, which was originally intended only to provide GPS timing accuracy to another measurement system.

3. Real-Time Equatorial Scintillation Analysis and Prediction

Work was begun during this year under Task 7 to develop techniques and software that would use near-real-time observations of scintillation from receivers deployed by PL/GPIA and of the topside ionosphere from the DMSP SSIES sensor package to produce short-term predictions of scintillation occurrence in a specified geographic region. The software developed is to be part of the Scintillation Decision Aid (SCINDA) program. This work focused on four activities:

1. Review the status of SSIES data processing at 50WS to determine whether further processing will be required to prepare the data for the analysis technique developed by P. Sultan [*Sultan,* 1996].
2. Establish procedures for calculating estimates of the height-integrated irregularity strength, C_kL, from the scintillation observations and implement them in software.
3. Determine how best to incorporate a wide range of ionospheric measurements into the equatorial C_kL model in WBMOD.
4. Develop software that implements the techniques developed for incorporation of real-time observations and generates grid-output files of ionospheric irregularity parameters and of S_4 for a particular scenario.

3.1. SSIES Data. The objectives of this subtask were to determine (1) if modifications made to the SSIES processing software by NWRA after formally delivering the code to Air Weather Service (AWS) in 1987 had been implemented as reported to AWS, and (2) if the one-second average ion densities output by the Scintillation Meter (SM) processing code were usable in P. Sultan's analysis algorithm. Comparison of the operational software used at 50WS with the code used at NWRA disclosed that several changes recommended by NWRA had not been implemented in the 50WS code. Consequently, updated versions of four subroutines in the SSIES processing code (routines SMPRC, ELAMP, RANGE, and FND511) again were provided to 50WS. A new routine, RNGANL, was also provided to generate a simple analysis of the embedded range flags found in a given pass which can be used to establish the validity of a look-up table used by the processing code to translate these range flags to settings of the electrometer and wide-band ranging electrometer amplifiers. Copies of these codes were also provided to Dr. Fred Rich (PL/GPSG).

Agreement was reached on the format of processed SSIES SM data to be provided NWRA by 50WS to meet the second objective of this subtask. NWRA will be sent data from the F-13 satellite for a 24-hour period to perform an assessment of whether any pre-processing of the data will be required prior to passing the data to P. Sultan's analysis algorithm.

3.2 Convert S_4 to C_kL. Software was developed to convert observations of intensity scintillation expressed in the S_4 scintillation index to estimates of the height-integrated irregularity strength, C_kL. This software was based on similar software developed for AWS as part of the Ionospheric Scintillation Specification and Prediction System (ISSPS). One of the ISSPS programs, GBCKL, was designed to take phase and intensity scintillation observations from modified GPS receivers and convert them to estimates of C_kL [*Secan et al.*, 1990]. The code delivered on this project, S4CKL, is a subset of the algorithms from program GBCKL. Figures 3 and 4 demonstrate the results obtained from this code using data from PL/GPIA receivers located at Antofagasta, Chile, and Ancon, Peru. These figures show data from five different paths: two VHF paths from Antofagasta westward to FLEETSAT-7 (first panel in each figure), an L-band path from Antofagasta northward to GOES-8 (second panel), a VHF path from Antofagasta eastward to FLEETSAT-8 (third panel), and a VHF path from Ancon westward to FLEETSAT-7 (fourth panel). The code was delivered to PL/GPIA for incorporation into the SCINDA program.

3.3 Use of Real-Time Observations. Two sources of real-time observations are to be incorporated into the SCINDA program: (1) intensity scintillation observations in the form of the S_4 scintillation index from three stations in the South American sector (Ancon, Peru; Antofagasta, Chile; and Howard AFB, Panama), and (2) estimates of the probability that post-sunset plume structures will form based on analysis of data from the SSIES SM sensor. These data are to be used to establish the location and severity (in terms of irregularity strength) of post-sunset plume structures in the region of interest (the South American equatorial sector for the purposes of this study) and to adjust the WBMOD climatology where no plume observations are possible based on observed scintillation levels. In the division of responsibilities, NWRA was given the task of developing algorithms and software to modify the WBMOD climatology to match the SSIES analyses and any available S_4 observations and to use this modified climatology to build gridded fields of irregularity and scintillation parameters into which the SCINDA program will place discrete plume structures based on models and analyses developed by other agencies.

In all, there are three types of inputs available: (1) specifications and surrogate measures of general solar and geophysical conditions (sunspot number, geomagnetic indices, season, *etc.*), (2) specifications of the probability that depletion plumes will form in the post-sunset equatorial ionosphere from analysis of DMSP SSIES data, and (3) real-time estimates of C_kL from the PL/GPIA receivers in the South American sector. If only the various indices are available, the fields output by the software described in the next section are based solely on the most recent WBMOD climatology [*Secan and Bussey,* 1993, 1994]. If real-time observations are available, this climatology is modified to reflect the observed conditions as follows:

1. If only an SSIES analysis is available and is determined to be valid for the time and location of the prediction (as discussed later), it will be used to set the position in the WBMOD climatological distribution of C_kL to either the plume or nonplume populations depending on whether the analysis value generated was above or below 0.5, respectively. All spatial and temporal variations will be derived from the underlying climatology.

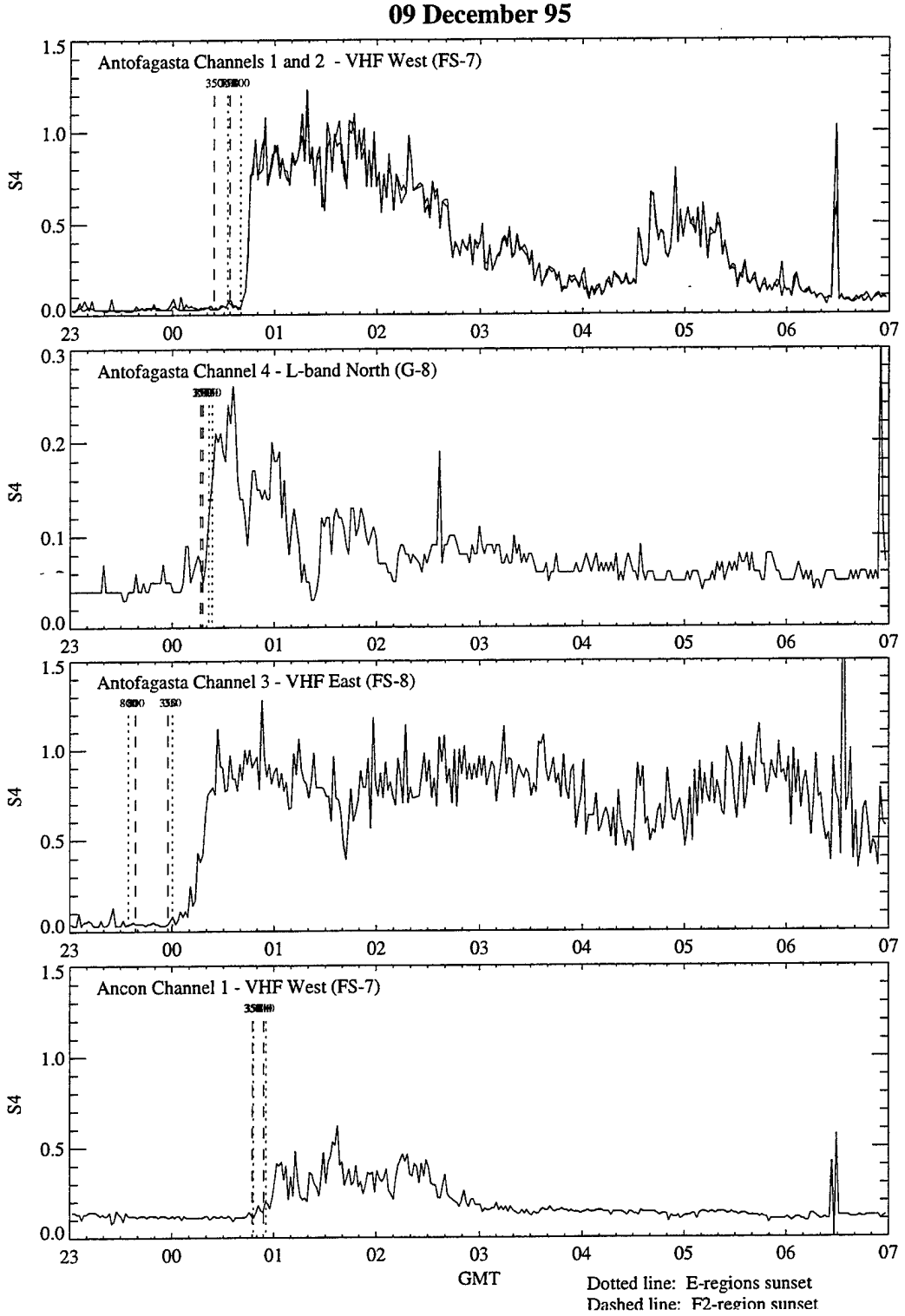

Figure 3. Examples of the S_4 intensity-scintillation index observed at Antofagasta, Chile, and Ancon, Peru, on four VHF and one L-band propagation path. The vertical dashed and dotted lines indicate times of E- and F-region sunset, respectively, for ionospheric penetration at 350 and 800 km altitudes.

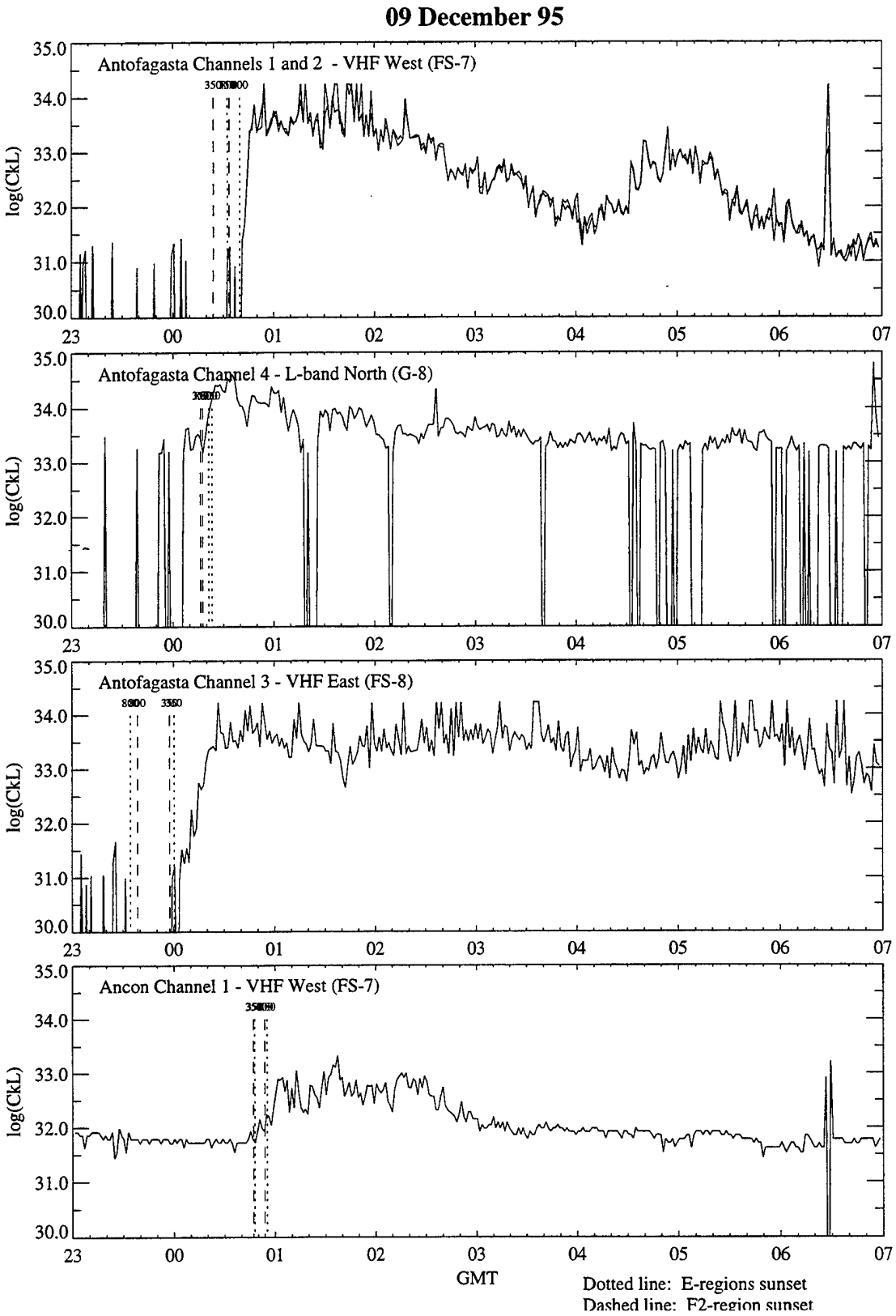

Figure 4. Time-series records of $\log(C_kL)$ calculated from the S_4 records shown in Figure 3 using the S4CKL program.

2. If C_kL values are input, they will be used to adjust the latitude variation of C_kL in the regions outside the real-time analysis region (defined as that region within which the SCINDA code will be placing plume structures based on its analysis of the real-time data). Inside the real-time analysis region, C_kL will be set to the nonplume C_kL value, which is either explicitly input to the analysis or derived from the nonplume WBMOD population.

Details of the use of each of these two types of real-time inputs follow.

3.3.1 SSIES Analyses. Two issues needed to be resolved in determining how to use P. Sultan's SSIES analysis in the real-time update process: how to modify the output fields based on the analysis (at this point a simple 0.0 or 1.0), and how far in time and space to extrapolate the analysis. The analysis is used to select which of the two populations in the $\log(C_kL)$ distribution function to use in generating the output C_kL fields. As stated earlier, if the input analysis is < 0.5, the C_kL value representative of the non-plume population is used; if the analysis is > 0.5, the value representative of the plume population is used. This is implemented by limiting the distribution function to a single Gaussian distribution, setting the $\log(C_kL)$ value at the peak of this distribution to either the non-plume or plume value generated by the rest of the model, and setting the percentile to use in generating C_kL from the distribution to 50%. Thus, the analysis is an "on-off switch" that will control whether the climatology sections of the output field are based on the plume or non-plume distributions.

Extrapolating the results of the SSIES analysis in longitude is complicated by the fact that conditions affecting the possible generation of plume structures vary with longitude. Thus, while an SSIES analysis at one longitude might indicate that conditions are good for plume generation, this might not be the case at longitudes not too far removed from the observation longitude, due to significant changes in factors that affect plume growth. In particular, the longitude variation of the seasonal modulation of plume generation in WBMOD is based on a hypothesis put forward in *Tsunoda* [1985] that plume generation will be most likely at those times of year when the sunset terminator is aligned with the local geomagnetic meridian. In addition, recent modeling work (such as in *Maruyama* [1988] and *Kelley and Maruyama* [1992]) suggests that the component of meridional neutral wind along the geomagnetic meridian can have a "braking" effect on the growth of plumes. This will also vary in some way with the local geomagnetic declination angle near the equator. Given this, we have decided to permit only limited extrapolation of SSIES analyses in longitude sectors where the geomagnetic declination angle varies significantly with longitude and between sectors, and to permit unlimited extrapolation in sectors where the declination is fairly constant in longitude.

Figure 5 illustrates this point and shows the division of the equatorial region into six longitude sectors. Unlimited extrapolation is permitted in sectors 1, 3, and 5; extrapolation is permitted by up to 15° in longitude in sectors 2, 4, and 6; and extrapolation of up to 5° in longitude is permitted from one sector to the next.

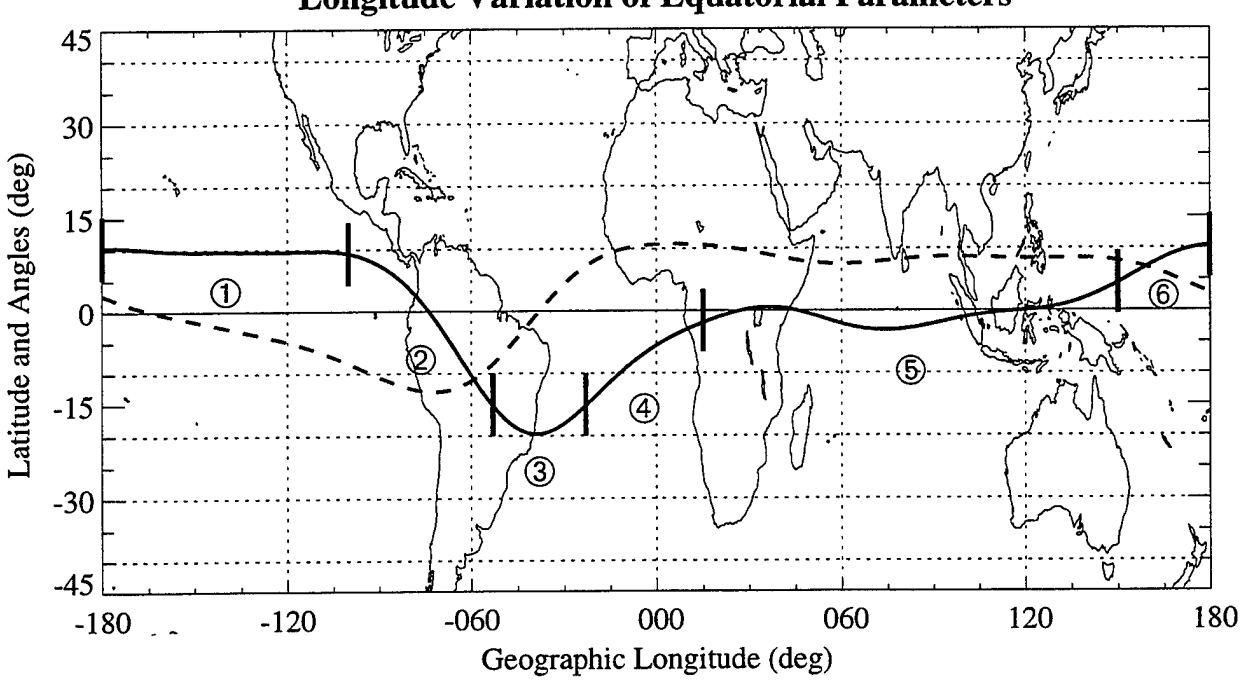

Figure 5. Longitude variation of the apex (dip) equator (dashed line) and the magnetic declination at the equator (solid line). The heavy vertical lines indicate boundaries between the six longitude sectors used in the SSIES analysis.

3.3.2 C_kL Observations. The use of the C_kL observations is more complex than the use of the SSIES analyses, and is less general in that it is tailored so that it expects the inputs to come from a particular set of locations (in geomagnetic latitude). In its current implementation, it expects to have observations from an equatorial station near the dip equator (Ancon, Peru), an equatorial station near to and equatorward of the anomaly crest region (Antofagasta, Chile), and a mid-latitude station near to and poleward of the anomaly crest region (Howard AFB, Panama). The program looks for observations at geomagnetic latitudes near to +2° (Ancon), -9° (Antofagasta), and +20° (Howard AFB). (In this context, "near" is within ±3° latitude.) These data are used to scale the latitude variation of C_kL in the sections of the grid that are outside the real-time analysis region (*i.e.*, at those grid points where the real-time analysis flag is zero).

The algorithm is expecting that the C_kL observations provided by the SCINDA program are the characteristic C_kL values for the time indicated on the input. They are used to set the maximum C_kL in the post-sunset region at the equator and at the anomaly crest. The program divides the inputs into day and night observations (based on the time-past-sunset time used in WBMOD) and into equatorial and near-crest observations. In each latitude regime, the maximum nighttime C_kL is selected from the inputs and is used as the maximum post-sunset value. The same is done with the daytime values.

The following algorithms are used, depending on what data are available.

1. If daytime equatorial values are available, set the daytime C_kL to the average of the two equatorial stations.

2. If nighttime values are available from both equatorial stations, adjust the C_kL levels at the equator and at the anomaly crest and the half-width of the transition function between the peak of the crest and the equator. If this analysis fails, the average difference in $\log(C_kL)$ between the observations and the model values are used to scale the latitude variation as an additive adjustment to both the equatorial and crest maximum values.

3. If a nighttime value is available from only one equatorial station (Ancon or Antofagasta), the difference in $\log(C_kL)$ between the observation and the model value is used as an additive adjustment to both the equatorial and crest maximum values.

4. If a nighttime value is available from the mid-latitude, near-crest station (Howard AFB), it is used to set the transition half-width from the peak of the anomaly crest into the mid-latitude ionosphere.

In all cases, the time variation both prior to and after the post-sunset peaks is controlled by the diurnal model from WBMOD.

It is important to note that the use of ground-based C_kL measurements is, in the current implementation, not generally applicable to any set of observations from any location or set of locations. Two constraints have driven the decision to implement to a specific set of inputs: limited resources for the development effort and limited spatial coverage by the planned ground-based observing network. The first constraint is self-explanatory – developing a general methodology that is robust in all situations is far more costly in development time (and in testing and debugging the implemented code) than developing one tailored to a specific set of inputs and situations. We have, however, striven to implement the codes in program IRRGRID so that future upgrades to more general capabilities are straightforward. The second constraint has to do with the latitude spacing of the expected observation set (Ancon, Antofagasta, and Howard) and the latitudinal structure of the equatorial region.

Figure 6 shows the latitude variation of $\log(C_kL)$ from the present WBMOD for the time of maximum scintillation activity (roughly an hour after sunset) near solar maximum. The vertical lines indicate the latitudes (solid lines) and corresponding conjugate latitudes (dashed lines) for each of the three stations that will be collecting data. While it is arguable whether the latitude variation will look exactly like this, the general distribution of a peak located at the equatorial anomaly, dropping off rapidly into mid-latitudes and more slowly towards the equator, is a reasonable one. The point to be made here is that while we may be able to determine that there is enhanced scintillation levels at the peaks from the measurements made at Antofagasta, it will be impossible with these data to (a) specify the latitude location of the peak and (b) specify the maximum $\log(C_kL)$ at the peak. In the sense of attempting to fit a model to a set of observations, this is a classic underdetermined, or undersampled, problem.

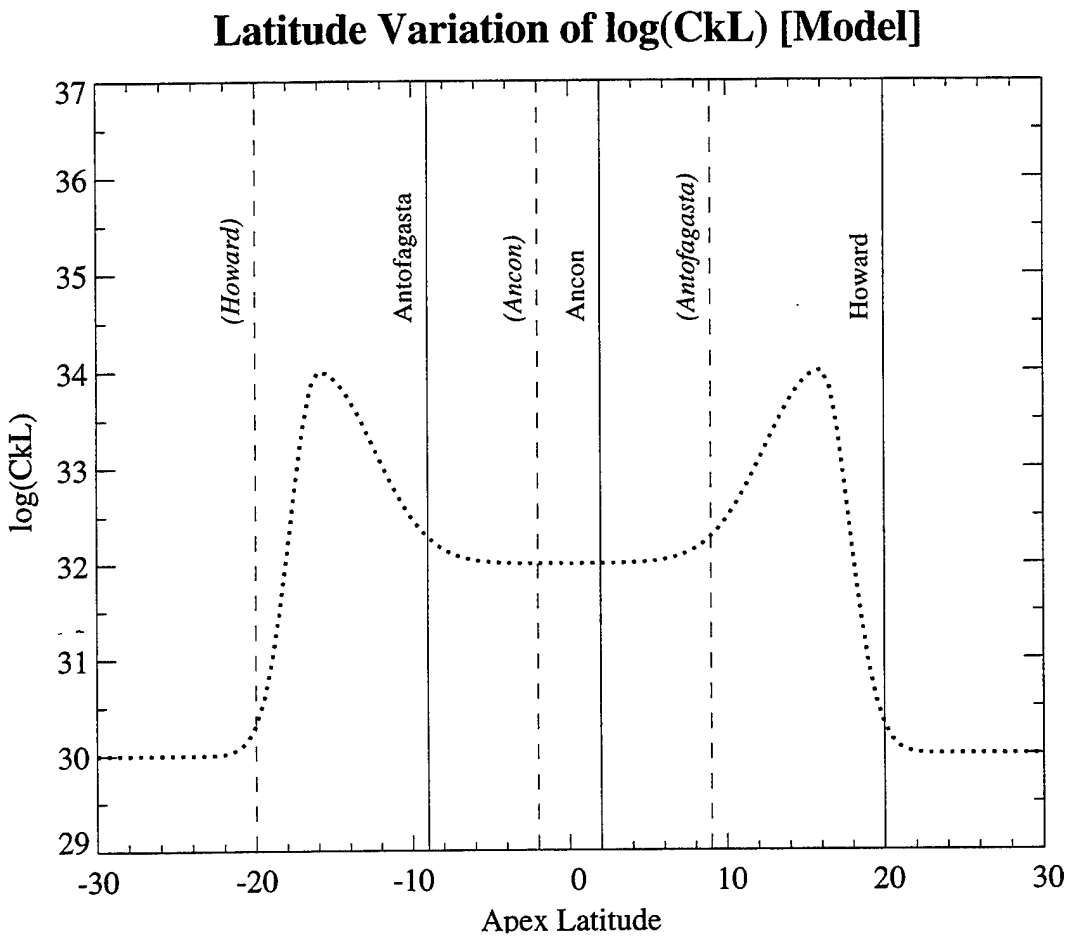

Figure 6. Latitude variation of $\log(C_kL)$ across the geomagnetic equator for solar maximum conditions in the post-sunset local-time sector. Vertical solid lines indicate the latitudes at which scintillation observations will be made, and vertical dashed lines indicate the corresponding conjugate latitudes.

A typical approach to solving such problems is to make use of as much *a priori* information as possible to constrain the problem so as to render it tractable. In our case, we have chosen to fix the location of the latitude peaks at the WBMOD values of ±16° geomagnetic latitude and to limit the value of $\log(C_kL)$ at the peak to a maximum value of 36.5 ($C_kL = 3.16 \times 10^{36}$). We then use the information from the stations to specify conditions at/near the geomagnetic equator (Ancon), near the anomaly crest on the equatorward side of the peak (Antofagasta), and near the anomaly crest on the mid-latitude side of the peak (Howard). The measured C_kL values are then used to adjust the model values for $\log(C_kL)$ at the equator and the peak (cross-equator symmetry is assumed) and the transition half-widths of the Gaussian functions used to model the latitude variation at the peaks.

A major upgrade to this analysis would be possible, given data to provide better resolution of the latitude variation. Potential candidates are the latitude variation of TEC through the area of interest output from a PRISM analysis or direct observations of TEC and, if possible, scintillation

from a low-altitude polar-orbiting satellite. It would be straightforward, though not trivial, to add the capability to use this information in the IRRGRID program, but it would require a bit of development work "up front" to determine how best to use observations of the latitude variation of TEC to model the expected latitude variation of scintillation in the post-sunset equatorial region.

3.4 WBMGRID Software. The algorithms described in the previous section were implemented in a set of four computer programs collectively named WBMGRID. The four programs have a simplified user interface, which reads inputs from a single ASCII-format file that can be constructed either manually via a text editor or automatically by a more sophisticated graphical user interface (GUI) program. Functionally, the WBMGRID programs (1) define a grid of geographic locations that will form one end of a set of ground-to-geostationary-orbit ray paths (program LLGRID), (2) calculate various geometry-related parameters used in the scintillation calculations along each ray path (program GEOMGRID), (3) calculate eight ionospheric plasma-density-irregularity parameters for each ray path based on the WBMOD climatology updated with real-time observations (program IRRGRID), and (4) calculate the S_4 intensity-scintillation index along each ray path (program S4GRID). Aside from software design considerations, the functions performed by the WBMGRID suite were divided among several programs for three reasons: (1) to make definition of the grid on which the calculations are made independent of all other calculations (program LLGRID), (2) to isolate CPU-intensive calculations that need be done only once for a given scenario (program GEOMGRID), and (3) to separate generation of the ionosphere (program IRRGRID) from the propagation calculations (program S4GRID) to permit other programs to alter the ionospheric parameters (primarily C_kL) based on analysis of data not available to or usable by program IRRGRID. [Note: A User's Manual has been written for the WBMGRID codes and is included as Appendix B to this report. Details such as input-data and file formats are provided there. The discussion in the remainder of this section will focus on design issues and on general use of this suite.]

Figure 7 shows the flow of information within the WBMGRID system for a sample implementation within the SCINDA framework. In this implementation, all interaction between the WBMGRID programs and the user are through the SCINDA interface. The SCINDA interface will interact with the user (a 50WS forecaster) to determine the parameters of a given run. It then obtains the necessary data from the 50WS database system and, if data are available, runs the Sultan analysis of the SSIES SM data and generates the necessary C_kL values from the S_4 observations made at Antofagasta, Ancon, and Howard AFB. This information is used to generate the (ASCII-format) inputs file for the WBMGRID suite (see Appendix B for details) that defines which of the programs are to run and provides the inputs necessary for each program (shown in Figure 7 as file wbminputs.dat). Assuming that the codes are running on a Unix system, SCINDA then starts a shell script that runs the various WBMGRID programs.

If the user has defined a new scenario (a different grid or satellite location), programs LLGRID and GEOMGRID will need to be run first to build the grid-definition file (shown in Figure 7 as file grid.bin) and the two geometry grid files (files geom.bin and eqgeom.bin). Program LLGRID will define the grid used by the other three programs either from specifications of the boundary and spacing of the grid in the inputs file or as an explicitly defined grid (one entry per grid-point location) in an optional (ASCII-format) input file (file grddef.dat). If the user has requested that a

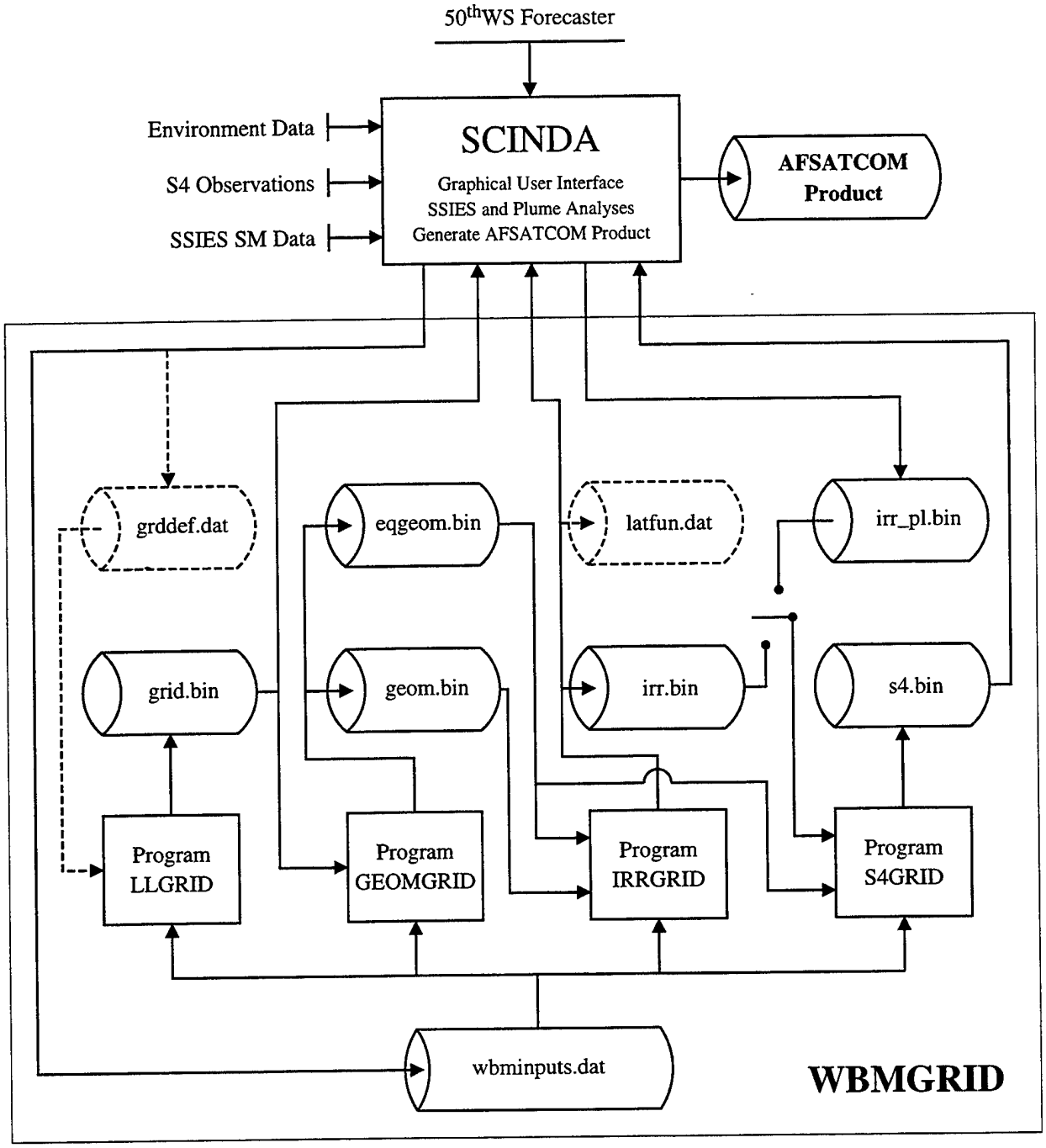

Figure 7. Flow diagram of the WBMGRID software in a sample implementation as part of the SCINDA system. Shaded programs and output files need be run only if the scenario geometry changes (*i.e.*, different grid, different satellite location). Dashed items are optional.

previously defined scenario be used (*i.e.*, one for which files grid.bin, geom.bin, and eqgeom.bin have been built and saved), then programs LLGRID and GEOMGRID need not be run.

The next step in processing is to run program IRRGRID to build the file containing the parameters that define ionospheric plasma-density irregularities for the propagation calculation

(file irr.bin). An optional output from this program, controlled by flags in the inputs file, is an (ASCII-format) output file that contains the latitude profile of $\log(C_kL)$ based on the other inputs to the IRRGRID program (file latfun.dat). These two files (irr.bin and latfun.dat) can then be read by the SCINDA program for the next step, which is to add the effects of discrete plume structures to the predicted C_kL grid. The updated grid of irregularity parameters can then be output to a file with the same format as irr.bin (file irr_pl.bin).

The final processing within the WBMGRID suite is to run program S4GRID to calculate S_4 for each grid point based either on the grid of irregularity parameters generated by program IRRGRID or by the modified file built by SCINDA. The file built by S4GRID (s4.bin) can then be reformatted as necessary by SCINDA to generate the final product for the end customer (AFSATCOM in this example implementation).

In the operations scenario just presented, program SCINDA would start the shell script that runs the WBMGRID programs twice. In the first run, programs LLGRID and GEOMGRID would be run if necessary, and program IRRGRID would be run to build the file of irregularity parameters. Program S4GRID would not be run at this time, which is accomplished by disabling the program via a flag in the inputs file (see Appendix B). (Note: If it is not necessary to run LLGRID and GEOMGRID, these are disabled in similar fashion.) When SCINDA has completed its update to the irregularity-parameter grid, the shell script is rerun with a new inputs file that has the run flags for all programs except S4GRID disabled. If the user desires that grids be generated for a series of times, this series of operations is repeated for each time desired. The files built for the different times can be differentiated by using the valid date/time in the name of each file (input and output file names are specified to each program in the inputs file – see Appendix B).

All the code in the WBMGRID suite is written in FORTRAN 77 with a minimal number of extensions to the ANSI standard. All four programs have been compiled and run on Unix (Sun workstation) and Windows (MS Windows 3.11) operating systems. The inputs file uses a NAMELIST-like protocol and grammar, but is controlled by a library of routines that are completely portable between compilers (which NAMELIST is not).

The size (lines of code and executable size) and run times (CPU) for each of the four WBMGRID programs are given in Table 3. These codes were compiled (using -O3 optimization) and run on a Sun UltraSPARC 140 workstation (Solaris 2.5) on a 1° by 1° latitude/longitude grid centered on (0.0° N, 275.0°E) with a minimum elevation of 10° and north and south latitude limits of 60°. The resulting grid contained a total of 16,027 grid points (10,985 in the equatorial region which require calculation of the equatorial geometry parameter in file eqgeom.bin). The inputs for program IRRGRID from the inputs file for this run are listed in Figure 8. These statistics are for the initial-release version (Version 0.00) of these codes dated 11 June 1996. In benchmark tests, we have established that a Silicon Graphics Indigo with a 150 MHz 440 CPU is slower than a Sun UltraSPARC 140 by a factor of 0.5 (SGI times = 2.0 × Sun times). The sizes of the various binary files generated in this run are listed in Table 4.

```
----  Environment Information  ----
Date = 960320
Time = 0200
F10 = 120.0
Kp = 3.0
Percentile = 90.0
----  R/T Data (from analyses)  ----
RT_Longitude_Limits = 260.0 305.0
Analysis_Longitude = 280.0
-- SSIES Analysis Results
SSIES_DateTime = 960320 013453
SSIES_Kp = 4.0
SSIES_Longitude = 305.0
SSIES_Analysis = 0.75
-- CkL Observations
NonPlume_CkL = 1.32E29
CkL_Observations_Table
960302 1211 -14.35 225.15 1.52E33
960302 1212  15.35 226.15 2.62E33
960302 1213  -2.35 227.15 3.72E33
END_OF_TABLE
----  CkL Latitude Function Output File ----
CkL_Latitude_File = lckl_v_lat.dat
```

Figure 8. Inputs to program IRRGRID for the test run summarized in Table 3.

Table 3. WBMGRID suite program statistics.

Program	Lines	Size	Run Time (sec)
LLGRID	3,427	109 kB	<1
GEOMGRID	5,924	144 kB	57
IRRGRID	13,145	253 kB	4
S4GRID	3,720	111 kB	<1

Table 4. WBMGRID suite file sizes (test example).

File	Size (kB)
grid.bin	454
geom.bin	1,297
eqgeom.bin	711
irr.bin	584
s4.bin	65

4. Publications

Bishop, G. J., A. J. Mazzella, Jr., and E. A. Holland, Application of SCORE techniques to improve ionospheric observations, *Proceedings of ION GPS-95,* Institute of Navigation, Alexandria, VA 1995.

Bishop, G. J., A. J. Mazzella, Jr., and E. A. Holland, A new algorithm to control DGPS measurement errors in both base stations and navigation receivers, and simplify WAAS error modeling, *Proceedings of ION GPS-95,* Institute of Navigation, Alexandria, VA 1995.

Bishop, G. J., A. J. Mazzella, Jr., E. A. Holland, and S. Rao, An overview of ionospheric effects and mitigation in RF communications, navigation and surveillance, presented at Ionospheric Effects Symposium (IES-96), Alexandria, VA, 1996.

Bishop, G. J., E. J. Weber, A. J. Mazzella, Jr., E. A. Holland, S. Rao, and P. Ning, Simultaneous TEC decreases and scintillation observed on GPS signals traversing equatorial plasma depletions, presented at Ionospheric Effects Symposium (IES–96), Alexandria, VA, 1996.

References

Bishop, G. J., E. J. Weber, A. J. Mazzella, Jr., E. A. Holland, S. Rao, and P. Ning, Simultaneous TEC decreases and scintillation observed on GPS signals traversing equatorial plasma depletions, presented at Ionospheric Effects Symposium (IES–96), Alexandria, VA, 1996.

Fremouw, E. J., C. C. Andreasen, and J. A. Secan, Investigations of ionospheric Total Electron Content and scintillation effects on transionospheric radiowave propagation, *Proposal NWRA–CR–94–P223,* Northwest Research Associates, Inc., Bellevue, WA, 1994.

Kelley, M. C., and T. Maruyama, A diagnostic model for equatorial spread *F*, 2. The effect of magnetic activity, *J. Geophys. Res., 97,* 1271-1277, 1992.

Maruyama, T., A diagnostic model for equatorial spread *F*, 1. Model description and application to electric-field and neutral wind effects, *J. Geophys. Res., 93,* 14,611-14,622, 1988.

Secan, J. A., M. P. Baldwin, and L. A. Reinleitner, Real-Time Scintillation Analysis System, Volume 1: Technical Description, *NWRA-CR-89-R049,* Northwest Research Associates, Inc., Bellevue, WA, 1990.

Secan, J. A., C. C. Andreasen, E. J. Fremouw, E. A. Holland, and A. J. Mazzella, Jr., Analysis of Ionospheric Monitoring System (IMS) Total Electron Content (TEC) data and equatorial phase-scintillation data, *Report PL–TR–95–2116,* Phillips Laboratory, Hanscom AFB, MA, 1995. **ADA306451**

Secan, J. A., and R. M. Bussey, An investigation of methods for improving models of ionospheric plasma-density irregularities and radio-frequency scintillation, *Report PL-TR-93-2260,* ADA278568, Phillips Laboratory, Hanscom AFB, MA, 1993.

Secan, J. A., and R. M. Bussey, An improved model of high-latitude F-region scintillation (WBMOD Version 13), *Report PL-TR-94-2254,* Phillips Laboratory, Hanscom AFB, MA, 1994. **ADA288558**

Sultan, P., Satellite signatures of the global occurrence morphology of equatorial spread F, presented at Ionospheric Effects Symposium (IES–96), Alexandria, VA, 1996.

Tsunoda, R. T., Control of the seasonal and longitudinal occurrence of equatorial scintillations by the longitudinal gradient in integrated E region Pedersen conductivity, *J. Geophys. Res., 90,* 447-456, 1985.

This page left blank intentionally.

Appendix A: Initial Shemya GPS Receiver/Radar Interference Summary

Abstract

* Site visit indicated presence of interference during radar operation.

* RF filter installation appeared to reduce interference.

* Test equipment was left operating, with remote dialup access for extension of study (especially with RF filter).

* Observed phenomena:

  Large, but stable, multipath at low elevations,

  Pulse trains in the Differential Group Delay, sometimes correlated with radar operations,

  Spikes in the Differential Group Delay, with no apparent correlation among satellites or with radar operations.

Background This initial review consisted of two days of operation of the GPS receiver system without an RF filter (3-Apr-96, 4-Apr-96), and four subsequent (but not successive) days with a dual-band bandpass filter (5-Apr-96, 7-Apr-96, 8-Apr-96, 9-Apr-96). The coverage for each of the days was not necessarily complete over time or observable GPS satellites, but is a substantial portion of the available GPS observability. The first three days of this survey constituted the Preliminary Shemya Site Study, which was performed during and immediately following the test equipment installation visit to Shemya (Eareckson) in April 1996, while further days of data were retrieved and processed subsequent to the site visit, using the equipment and software established at the radar site during the visit.

Noise bursts The predominant effect seen during periods of radar operation without a receiver RF filter was a set of noise bursts in the Differential Group Delay (DGD), straddling the stated radar test period (presumably due to the warm-up period for the radar). The amplitude of these bursts ranged from about 20 TEC units to about 100 TEC units, with different amplitudes for different satellites, even during the same radar test.

With the installation of the RF filter, effects were still observed in the DGD signals during radar tests, but these appeared as distinct pulse trains, ranging in amplitude from 20 TEC units to 100 TEC units, with a pulse interval of about 3 to 10 minutes. However, these pulses did not appear on all satellites, and had different amplitudes and different numbers of pulses for different satellites even during a single radar test event. It is not even certain that the individual pulses are coincident for different satellites.

It was also noted that a pulse-train interference effect was observed on occasions when there was no radar activity reported to us. These were basically of the same nature as those cases where the radar was known to be operational, except that the pulse amplitudes were sometimes observed to be as large as about 200 TEC units.

For reference, the radar operation times (UT) known to us are listed for each of the relevant days.

3-Apr-96	4-Apr-96	5-Apr-96	7-Apr-96	8-Apr-96	9-Apr-96
3:47	8:48	10:05	9:16	8:51	8:27
9:12	10:29	20:26	21:18	19:37	10:08
21:15				20:53	20:29

The periods marked by noise bursts or pulse trains with no known radar operations are listed below. The times are also Universal Time, but are only approximate because the observed events are not instantaneous.

3-Apr-96	4-Apr-96	5-Apr-96	7-Apr-96	8-Apr-96	9-Apr-96
16:20				22:30-	0:30
17:10				24:00	3:15
					4:20-5:30

Based upon discussions with on-site personnel, these pulse train features are unlikely to be associated with the radar operation, but rather arise from ancillary equipment that is utilized during the radar tests and also at other times.

Spikes. A significant feature seen sporadically in the recorded data is a large spike or pulse which is isolated from other effects, but is sometimes associated with the acquisition or loss of a satellite and occasionally associated with a subsequent data dropout. A spike appears to be a single wild data sample (at a 6-second sampling interval), while a pulse is distinctly composed of many data samples.

The spikes or pulses do not appear on multiple satellites at their time of occurrence, and range in amplitude from about 50 TEC units (the typical limit of detectability) to about 450 TEC units. The presence of the RF band-pass filter does not appear to influence the occurrence of spikes, but further data collection without the RF filter would be needed to make a statistically significant comparison. The large spikes do not appear to be associated with the operation of the radar, but smaller ones sometimes do appear during radar events, possibly as the largest of several pulses in a pulse train becoming visible above the typical noise and multipath level.

Multipath. The multipath pattern appeared to be consistent over the first two days of data collection, even without the RF filter, so further days were not examined in detail for the consistency of this pattern. The incorporation of the RF filter had been examined previously at Hanscom, and was determined to have no deleterious effects on the GPS signals.

The DGD noise/multipath amplitude at low elevations is substantial, often on the order of 100-200 TEC units. The current provisions utilizing an elevation threshold for data acquisition may require re-evaluation of this parameter after the IMS is installed, with some associated change in the region covered by the observations.

Ongoing Investigations. Inquiries were conducted with regard to the operations of other equipment at the site, particularly those in the vicinity of the GPS antenna, to evaluate the possibility of interference sources that are distinct from, but often coordinated with, the radar operation. These discussions indicated that neither the radar nor other instrumentation on the roof of the radar building was the source of the interference, but that another activity was the source. Further details are expected at the time of the installation visit, when the antenna-siting evaluation will be concluded.

The influence of the extraneous effects on the phase-averaging process is being evaluated quantitatively, using techniques that have already been developed for other investigations. A preliminary determination for the elevation threshold will be part of this evaluation. Tentative conclusions are that only the very largest discrete events (spikes and pulses) will pose a long-term problem for phase-averaging, but the multipath may be a significant concern.

This page left blank intentionally.

Appendix B: WBMGRID User's Manual

The User's Manual written for the WBMGRID programs is attached as an appendix to this report.

This page left blank intentionally.

Overview

Four programs make up the WBMGRID code: LLGRID, GEOMGRID, IRRGRID, and S4GRID. Each of these programs reads user inputs from an ASCII-format file (or a collection of files), grid files generated by other programs "upstream" in the processing chain, and outputs one or more grid files containing processing results. The primary function of each program is as follows:

LLGRID: Generate a grid file containing the definition of the latitude-by-longitude grid to be used by later programs. This grid file is tailored to a single, user-specified geostationary satellite location.

GEOMGRID: Generate two grid files containing all static geometry information used by the ionosphere model in IRRGRID and the propagation model in S4GRID.

IRRGRID: Generate a grid file of the parameters used to characterize ionospheric plasma-density irregularities for the propagation model. This is based on climatology, climatology adjusted by an SSIES analysis, or climatology scaled by real-time observations.

S4GRID: Generate a file of S_4 values based on the irregularity parameters read from the file built by IRRGRID and modified by other codes (to add discrete plume structures).

These programs were designed so that the geometry of the scenario (as calculated by programs llgrid and geomgrid) need only be calculated when either the definition of the grid changes (spacing or latitude/longitude range) or the location of the satellite changes.

Subsequent sections will present the structure and contents of the inputs file, the output files, more detail on the processing and calculations made within each program, and the error behavior of the system.

Inputs File

User inputs to all four programs are controlled via a user interface library (UINLIB) which provides a NAMELIST-like protocol that is both flexible and portable. The library will allow input from either an external ASCII-format file or from the standard input, with the determination of the input source made via command-line inputs to the program (for a UNIX implementation). The general form for inputs are the keyword name of the input starting at the beginning of an input line followed by an equal sign (=) followed by one or more input values. In each program, some of the inputs are required, and others are optional. If an optional input is missing, the program will substitute a default value for that input. Comments may be placed in an inputs file by placing two minus signs (--) at the start of the line. Unlike the NAMELIST facility, input character strings (such as file names) are not enclosed in single quotes ('). Order of inputs within the file is arbitrary, with the exception of table input (see the discussion under program IRRGRID). All keywords must be spelled correctly, and with the correct case (upper or lower). Keywords cannot have embedded blanks, so several of them use the underscore character (_) for a blank.

The library is designed so that all inputs not recognized by a particular program are simply ignored. This permits the generation of a single inputs file that contains all inputs for a particular run of the entire set of programs. An example of an inputs file for a full run of all four WBMGRID programs is shown in Appendix A. A discussion of the inputs specific to an individual program will be postponed until the description of that program. There are, however, a number of inputs in this file that are common to all programs; these will be discussed here.

The following is an example of the inputs file that would be common to all programs:

```
-----------------------------------------
-----  General Inputs - All Programs   -----
-----------------------------------------
Inputs_File_Built = 03 June 1996 / 12:30:22 GMT
----  Run Control Information  ----
Run_llgrid = 1
Run_geomgrid = 1
Run_irrgrid = 1
Run_s4grid = 1
----  Diagnostic Print Control  ----
IO_DiagPrtFlag = 1
Proc_DiagPrtFlag = 0
----  Files Information  ----
Grid_File = grid_def.bin
Geometry_File = geom_def.bin
EqGeometry_File = eqgeom_def.bin
Irregularity_File = irrgrid.bin
S4_File = s4grid.bin
-------------------------------------
```

The contents, use, and (if any) defaults for each of these are as follows:

`Inputs_File_Built` : This is a character string that can have any format, but is designed to have the date and time that the inputs file was built, either by hand or as output from a GUI-based control program. This string is output by each program to standard output as soon as it is read. If this is missing, nothing is output.

`Run_llgrid` : This flag is used to control whether program LLGRID will run after reading this inputs file. If set to zero (0), the program will exit without further processing. If set to one (1), the program will continue and process normally. This permits the programs to be placed in a single "canned" execution script that never changes from run to run. Whether a particular program runs or not is controlled by flags in the inputs file. This will be discussed further in a later section that describes an implementation of these programs. [Default: 0 (no run)]

`Run_geomgrid` : Same as above for the GEOMGRID program.

`Run_irrgrid` : Same as above for the IRRGRID program.

`Run_s4grid` : Same as above for the S4GRID program.

`IO_DiagPrtFlag` : This flag controls the generation of diagnostic output concerning input and output operations. It is designed for use in debugging the programs or in tracking down execution errors

during operations. If set to zero (0), I/O diagnostic output is suppressed; if set to one (1), it is enabled. This input should either be set to 0 or left out entirely for operational use. [Default: 0 (print suppressed)]

`Proc_DiagPrtFlag` : This flag controls the generation of diagnostic output concerning all processing. It is designed for use in debugging the programs or in tracking down execution errors during operations. If set to zero (0), processing diagnostic output is suppressed; if set to one (1), it is enabled. This input should either be set to 0 or left out entirely for operational use. [Default: 0 (print suppressed)]

`Grid_File` : Name of the (binary) output file built by program LLGRID. [Default: `grid.bin`]

`Geometry_File` : Name of the (binary) output geometry file built by program GEOMGRID. [Default: `geom.bin`]

`EqGeometry_File` : Name of the (binary) output equatorial geometry file built by program GEOMGRID. [Default: `eqgeom.bin`]

`Irregularity_File` : Name of the (binary) output irregularity-parameters file built by program IRRGRID. [Default: `irrgrid.bin`]

`S4_File`: Name of the (binary) output S_4 file built by program S4GRID. [Default: `s4grid.bin`]

Binary Grid File Descriptions

The WBMGRID system uses one or more ASCII-format inputs files (one for each program or one for a run of the entire system), five binary-format grid files, an optional ASCII-format grid-definition input file, and an optional ASCII-format C_kL latitude-function output file. The inputs file was described in the last section, and the two optional ASCII-format files will be discussed under programs LLGRID and IRRGRID, respectively. The format and contents of the five binary-format grid files will be presented here.

All of the binary grid files have the same general format: a one-record (I/O record) header followed by grid-data I/O records. The headers contain file-verification information (ID flags and date/time generated information) and other information concerning the size and contents of the rest of the file. The grid-data I/O records contain entries for 100 grid points. The size of the I/O records are different for each file, as the size of the grid-point entries for each is different. Tables 1 through 5 in Appendix B describe the contents of the headers and I/O records for each of the five binary files defined to date (`grid.bin`, `geom.bin`, `eqgeom.bin`, `irrgrid.bin`, and `s4grid.bin`)

Program Descriptions

Program LLGRID

Program LLGRID constructs a file (`grid.bin`, see Table 1) that contains the latitude and longitude of each grid-point for which later programs will calculate their various parameters. This grid is defined as an equally spaced latitude-by-longitude grid centered (initially) on the latitude and longitude of the geostationary satellite to which the propagation paths lead. The bounds of the grid are defined initially by a minimum elevation angle, and can be further limited by input of minimum and maximum latitude and longitude values. In addition to the general inputs described earlier, the program-specific inputs to LLGRID are as follows:

Required Inputs:

`Satellite_Latitude` : Latitude of the geostationary satellite (degrees, +north).

`Satellite_Longitude` : Longitude of the geostationary satellite (degrees, +east).

`Satellite_Altitude` : Altitude of the geostationary satellite (km).

`Satellite_Velocity` : Satellite velocity vector (m/s). Three entries are required to define the velocity vector: (+north, +east, +down).

Optional Inputs:

`Latitude_Spacing` : Grid spacing in latitude (degrees) [Default: 1.0].

`Longitude_Spacing` : Grid spacing in longitude (degrees) [Default: 1.0].

`Minimum_Elevation` : Minimum elevation angle to define the edge of the coverage area (degrees) [Default: 10.0].

`Latitude_Limits` : Grid limits in latitude (degrees, +north). Two entries are required: southern edge and northern edge. Enter -999.0 to default either side to the limits set by `Minimum_Elevation`. [Default: -999.0 -999.0].

`Longitude_Limits` : Grid limits in longitude (degrees, +east). Two entries are required: western edge and eastern edge. Enter -999.0 to default either side to the limits set by `Minimum_Elevation`. [Default: -999.0 -999.0].

`Grid_Def_File` : Name of an ASCII-format input file containing information for each grid point to be used in calculations by the other WBMGRID programs. This information will be transferred to the binary-format grid-definition file. All other optional inputs will be ignored.

This last optional input permits a user to explicitly specify the latitude/longitude grid to be used rather than having LLGRID construct it from the other inputs. The format of this ASCII file is as follows (all lines are read using free-format input):

Line 1: `glat0 dlat glon0 glon npts`

`glat0` : Base latitude (most southerly latitude in grid (deg)

`dlat` : Latitude spacing (deg)

`glon0` : Base longitude (most easterly longitude in grid (deg)

`dlon` : Longitude spacing (deg)

`npts` : Total number of grid points in the file

Lines 2 through `npts+1`: `nlat nlon glat glon ghgt az el`

`nlat` : Grid-point latitude number

`nlon` : Grid-point longitude number

`glat` : Grid-point latitude (deg, north)

`glon` : Grid-point longitude (deg, east)

`ghgt` : Grid-point altitude (km)

`az` : Azimuth angle to satellite (deg, clockwise from north)

`el` : Elevation angle to satellite (deg)

Line `npts+2`: `-1`

The grid-point numbers are simply the number of latitude or longitude spacing steps the grid point is removed from the base latitude or longitude plus 1. Note that it is important that the directional information (elevation and azimuth angles) to the satellite from each grid point needs to be consistent with the satellite location input via the inputs file.

Program GEOMGRID

Program GEOMGRID constructs two files (`geom.bin` and `eqgeom.bin`, Tables 2 and 3 in Appendix B), which contain all necessary time-independent geometry parameters required by the irregularity-model and propagation calculations at each grid point specified in the file built by program LLGRID. Two files are generated in order to conserve space: not all grid points will require a number of the parameters that are used to drive the WBMOD C_kL model in the equatorial and anomaly crest regions. These parameters (as defined in Table 3 of Appendix B) are calculated only for those grid points within 35° of the dip equator. This program requires no information from the ASCII inputs file beyond the general inputs described earlier.

Program IRRGRID

Program IRRGRID constructs a file (`irrgrid.bin`, Table 4 in Appendix B) that contains the parameters that define ionospheric plasma-density irregularities at each point on the grid defined in the grid-definition file built by LLGRID. This code includes the models for these parameters from the WBMOD

program (Version 13.04) and algorithms to adjust or replace the climatology with information from real-time observations (described in a later section). Inputs to the program include the following:

Required Inputs:

`Date` : Date for the run (GMT; year, month, and day).

`Time` : Time for the run (GMT; hours and minutes).

`F10` : The 10.7cm solar radio flux (janskys).

`Kp` : 3-hour K_p geomagnetic index.

`Percentile` : Percentile in log(C_kL) PDF (percent). This is only used when the model is run strictly in climatology mode, *i.e.,* when there are no real-time data other than SSN and K_p.

Optional Inputs:

`Kp(SS)` : K_p at sunset. [Default: user-input K_p]

`Kp(SSJ4)` : Effective-K_p derived from SSJ/4 boundary observations. [Default: user-input K_p]

`Drift_Velocity`: The *in-situ* drift velocity of the irregularities (m/s). Three inputs are required to define the velocity vector: (+north, +east, +down). [Default: internal model] [Note: This input is currently for testing purposes only.]

Real-time Data Inputs:

`SSIES_DateTime` : The GMT date (YYMMDD) and time (HHMM) of an SSIES analysis, two entries separated by one or more blank spaces. This is defined as the time of the equator crossing for the pass from which the analysis was made. If this entry is missing from an inputs file, the program assumes there is no SSIES analysis available and will ignore the next three inputs if they are in the file.

`SSIES_Longitude` : Geographic longitude of the equator crossing from the pass used in the analysis (degrees east).

`SSIES_Analysis` : Results of the SSIES analysis. A number ranging from 0.0 (no plume development expected) to 1.0 (plume development expected). Details of how this is used will be presented later.

`SSIES_Kp` : The 3-hour K_p index valid at the time of the SSIES analysis (*i.e.,* at the equator-crossing time).

`RT_Longitude_Limits` : Geographic longitude limits of the region which is to be updated with real-time observations of equatorial plume structures (degrees east). Two values are input: the westernmost longitude followed by the easternmost longitude. These structures are added by the GUI control program. If there are not data available from which the structures can be generated, either do not include these in the inputs file or set both of these inputs to 0.0 to indicate that the program should generate the entire grid based on the WBMOD climatology (based on an SSIES analysis if one is available). [Note: These limits are converted to geomagnetic-longitude region boundaries by the program. Geomagnetic latitude boundaries are set internally to ±20°.] All grid points that are within the real-time analysis region will have C_kL values set to the non-plume C_kL

value (input described below) and will have the real-time flag in the `irrgrid.bin` and `s4grid.bin` files set to 1.

`Analysis_Longitude` : Geographic longitude centered on the location of the real-time scintillation observations that are to be used in the analysis (degrees east). If this is not input, it will be set to either (1) the longitude determine to be the center of the input observations, (2) the center of the real-time analysis region from the `RT_Longitude_Limits` inputs, or (3) set to the default, in that order. [Default: 280.0 degrees]

`NonPlume_CkL` : The C_kL observed outside plume structures. This value is used to "fill" the real-time analysis region. [Default: WBMOD values for the non-plume population]

`CkL_Observations_Table` : This keyword indicates the start of a table of C_kL values derived from real-time scintillation measurements. The format of this table is as follows:

```
CkL_Observations_Table
YYMMDD HHMM GLAT GLON CKL
YYMMDD HHMM GLAT GLON CKL
YYMMDD HHMM GLAT GLON CKL
YYMMDD HHMM GLAT GLON CKL
END_OF_TABLE
```

The latitude and longitude are the geographic (degrees +north and +east) coordinates of the 350 km ionospheric penetration point (IPP) of the propagation path on which the C_kL value was measured. This table can have up to 100 separate entries, and *must* be terminated by the `END_OF_TABLE` string. Details of what should be in this table and how the data are used will be presented later.

`CkL_Latitude_File` : Name of the C_kL latitude-variation output file. [Default: No output file]

If the last optional parameter is input, it will cause the program to build an ASCII-format output file that provides the variation of $\log(C_kL)$ with geomagnetic (apex) latitude in one degree steps from -20° to +20° at the time of peak scintillation levels as defined by the WBMOD model (approximately 1.5 hours after local sunset). The variation is based on the analysis of the real-time SSIES and scintillation data used in producing the output grid file. This file has a two-line header labeling the columns followed by two columns with the geomagnetic (apex) latitude and the $\log(C_kL)$ value at that latitude. If this file-name parameter is not present in the inputs file, this file will not be constructed. An example of this file is given in Appendix B.

The real-time analysis flag output to the grid file (and included in the S4GRID output file) is an indicator of whether a grid point falls within the region where analysis of real-time scintillation observations are to be used to place plume structures. This flag will be useful for generating a display of the fields in the grid files that differentiates between regions where the analysis is based on climatology and those that are based on observed structures. This region is bound on the east and west by the geomagnetic longitudes passing through the longitudes specified by the `RT_Longitude_Limits` input by the user and on the north and south by ±20° geomagnetic latitudes. Note that this flag has nothing to do with whether real-time C_kL measurements were used to scale the WBMOD-based values outside the region where plume structures are to be placed. It is solely to be used in later display of the grids.

Program S4GRID

Program S4GRID constructs a file (`s4grid.bin`, Table 5 in Appendix B) that contains the S_4 values calculated from the irregularity parameters in the file built by IRRGRID. The program uses the propagation code from the WBMOD program (Version 13). Inputs to the program are as follows :

Required Inputs:

`Frequency`: System frequency (MHz).

Use of Real-Time Inputs

Input of real-time observations to the WBMGRID programs is either via the inputs file to program IRRGRID or through input of a modified grid of C_kL values to program S4GRID (*i.e.*, by introducing discrete plume structures in the `irrgrid.bin` file after it has been generated by the IRRGRID program and before S4GRID has been run). This section will discuss the real-time input options to the IRRGRID program.

There are two sources of real-time inputs to IRRGRID: estimates of the likelihood of plume production in the post-sunset equatorial region based on analysis of data from the DMSP SSIES sensor package, and estimates of the C_kL parameter calculated from ground-based scintillation measurements. Generation of the SSIES analysis and of the C_kL estimates are to be done by either the controlling GUI program, or by another program controlled by the GUI. Program IRRGRID expects these analysis and calculation to be completed, and the results input via the inputs file using the keywords as specified in an earlier section.

The use of real-time data within IRRGRID is as follows:

1. If no real-time data are input (SSIES or C_kL), the parameters output on the grid are based solely on the WBMOD climatology using the input F10.7 and K_p values. The real-time analysis flag output to the grid file (variable `irt`) will be set to zero at all grid points.

2. If only an SSIES analysis is input and is determined to be valid, it will be used to set the position in the climatological distribution of C_kL to either the plume (analysis value > 0.5) or the nonplume (analysis value < 0.5) populations. The WBMOD climatology will be used to set and vary all other parameters. The real-time analysis flag will be set to zero at all grid points *unless* a real-time analysis longitude range is input. In that case, this flag will be set to one within that range (see earlier discussion of this flag).

3. If C_kL values are input via the observations table, they will be used to adjust the latitude variation of C_kL in the regions outside the real-time analysis region. Inside that region, the C_kL will be set to the nonplume C_kL value (either explicitly input or derived from the nonplume WBMOD population). The real-time analysis flag will be set to zero outside the region and set to one inside it.

The IRRGRID program determines whether an input SSIES analysis is valid for the grid being constructed according to the following scheme:

1. : If any of the inputs are missing (date, time, longitude, K_p, analysis), don't use it.

2. : If the analysis is more than three hours old, don't use it.

3. : If the K_p input for the grid is more than 2 K_p-units different than K_p at the time of the SSIES analysis, don't use it.

4. : If the longitude difference between the analysis and the sunset terminator at the time of the grid is larger than a longitude-dependent distance, don't use it.

This last criterion is based on the longitude variation of the geomagnetic declination (basically the angle between the geographic and geomagnetic meridians at the equator) and the model for the effect of this variation on the probability of plume generation used in WBMOD. The full rationale for this is discussed in Appendix C, but the basic idea is that within longitude sectors where the declination is not changing appreciably with longitude the permitted longitude distance between the SSIES analysis and its application is larger than the size of the region. In sectors where the declination is changing rapidly with longitude, the longitude difference is limited to 15° of longitude. If the SSIES analysis and the sunset longitude are in different sectors, the difference is limited to 5°. A map showing the boundaries of the sectors can be found in Appendix C.

The use of the C_kL observations is more complex than the use of the SSIES analyses, and is less general in that it is expecting the inputs to come from a particular set of locations (in geomagnetic latitude). In its current implementation, it expects to have observations from an equatorial station near the dip equator (Ancon, Peru), an equatorial station near to and equatorward of the anomaly crest region (Antofagasta, Chile), and a mid-latitude station near to and poleward of the anomaly crest region (Howard AFB, Panama). The program looks for observations at geomagnetic latitudes near to +2° (Ancon), -9° (Antofagasta), and +20° (Howard AFB). (In this context, "near" is within ±3° latitude.) These data are used to scale the latitude variation of C_kL in the sections of the grid that are outside the real-time analysis region (*i.e.*, at those grid points where the real-time analysis flag is zero).

The program is expecting that the C_kL observations in the inputs file (in the `CkL_Observations_Table`) are the characteristic C_kL values for the time indicated on the input. They are used to set the maximum C_kL in the post-sunset region at the equator and at the anomaly crest. The program divides the inputs into day and night observations (based on the time-past-sunset time used in WBMOD) and into equatorial and near-crest observations. In each latitude regime, the maximum nighttime C_kL is selected from the inputs and is used as the maximum post-sunset value. The same is done with the daytime values.

The following algorithms are used depending on what data are available.

1. : If daytime equatorial values are available, set the daytime C_kL to the average of the two equatorial stations.

2. : If nighttime values are available from both equatorial stations, adjust the C_kL levels at the equator and at the anomaly crest and the half-width of the transition function between the peak of the crest and the equator. If this analysis fails, the average difference in $\log(C_kL)$ between the observations and the model values are used to scale the latitude variation as an additive adjustment to both the equatorial and crest maximum values.

3. : If a nighttime value is available from only one equatorial station (Ancon or Antofagasta), the difference in $\log(C_kL)$ between the observation and the model value is used as an additive adjustment to both the equatorial and crest maximum values.

4. : If a nighttime value is available from the mid-latitude, near-crest station (Howard AFB), it is used to set the transition half-width from the peak of the anomaly crest into the mid-latitude ionosphere.

In all cases, the time variation both prior to and after the post-sunset peaks is controlled by the diurnal model from WBMOD.

Sample Implementation and Use

Appendix A shows a sample inputs file and Unix script to run these programs. In this implementation, all of the inputs are in a single inputs file and all four programs are run every time. Whether a particular program actually runs through its entire processing cycle is controlled by the run flag in the inputs file. The inputs file is generated either by a user with a text editor, or by a GUI that interfaces with the user for input and then builds the inputs file and starts the script.

Consider the following operational scenario: every hour two forecast grids are generated for a fixed scenario (*i.e.*, a fixed geographic grid to a fixed satellite geometry) for one and two hours in the future. A GUI will control execution of the WBMGRID programs, and will also place discrete plume structures into the `irrgrid.bin` file (updating the C_kL parameters in the file built by program IRRGRID) and generate the final product that is sent to the customer. The WBMGRID codes would be run as follows:

1. : The GUI would be used by the operators to build the grid and geometry files once. The inputs file would have the run flags for programs LLGRID and GEOMGRID set to one (1) and the flags for programs IRRGRID and S4GRID set to zero (0). These files would not need to be rebuilt unless the scenario changes in some way. This can be done at any time prior to running the codes to produce the irregularity and S_4 files. The only inputs required in the inputs file are the general inputs and those for programs LLGRID and GEOMGRID.

2. : When a forecast is to be run, the GUI would build inputs files for the two forecast times (one and two hours in the future) and run program IRRGRID with both inputs files to build two `irrgrid.bin` output files, one for each forecast time

3. : When program IRRGRID has built the files, the GUI can then run the plume-generation software to modify the `irrgrid.bin` files to include these structures.

4. : When the plume-structure update is completed, the GUI can then run program S4GRID on both `irrgrid.bin` forecast files to generate the forecast `s4grid.bin` files. . The run flags for all programs except S4GRID are set to zero (0), and inputs for all programs other than S4GRID can be left out if desired (they will be ignored by S4GRID in any case).

5. : When program S4GRID has built the files, the GUI can then display them and generate any products from them.

Error Handling Procedures

All of the WBMGRID programs have been designed to fail-safe, by which we mean they will recognize error situations and exit from them in an orderly, graceful fashion. Typical failure modes are file errors (missing files, errors reading from or writing to files), parameter errors (missing parameters, misspelled keywords in the inputs file, missing parameters that are not optional), and calculation errors (logic or computation errors in the code). The first two modes are typically up to the user to correct in one way or another, the last mode will typically require intervention by a software analyst.

The general error-handling procedures in all four programs is to build an ASCII-format text file (`errorsum.txt`) describing the error and then terminating with a non-zero exit status. Prior to exiting, the content of the error-output file is printed in the standard output as well. An error message has the following format:

```
Error Number: N.NN / Program: PROGNAME
Message:  STRING
------------------------------------------------------------
    ---  Lines of additional explanatory information  ---
------------------------------------------------------------
```

where `N.NN` is the error number, `PROGNAME` is the name of the program in which the error was encountered, and `STRING` is a one-line explanation of the error. Between the two lines of minus signs are a variable number of lines of additional information. The first two lines in the file will always have the format shown here, which will allow a GUI running the codes to determine what sort of error was encountered and help the user rectify things.

At the present time, the following errors can be generated (by error number):

`1.xx` : Errors involving the inputs file.
`1.10` : The inputs file was missing (an error return from an attempt to open the file).
`1.20` : An error was encountered attempting to read the file (typically a format error).
`1.40` : An input parameter was in error (out of range, *etc.*).
`1.50` : A required parameter was missing from the inputs file.

`2.xx` : Errors involving a grid file (input or output).
`2.10` : The grid file was missing (an error return from an attempt to open the file).
`2.20` : An error was encountered attempting to read from the file.
`2.30` : An error was encountered attempting to write to the file.
`2.40` : A structure error was encountered (problems with the file format, header, *etc.*).
`2.50` : An end-of-file was encountered when one was not expected (the file was too small).

`3.xx` : Program errors (computational or logic)
`3.10` : An error condition was encountered involving internal program operation.

Actions to be taken are, at this time, TBD.

References

Kelley, M. C., and T. Maruyama, A diagnostic model for equatorial spread *F*, 2. The effect of magnetic activity, *J. Geophys. Res., 97,* 1271-1277, 1992.

Maruyama, T., A diagnostic model for equatorial spread *F*, 1. Model description and application to electric-field and neutral wind effects, *J. Geophys. Res., 93,* 14,611-14,622.

Tsunoda, R. T., Control of the seasonal and longitudinal occurrence of equatorial scintillations by the longitudinal gradient in integrated E region Pedersen conductivity, *J. Geophys. Res., 90,* 447-456, 1985.

Appendix A. Sample Implementation

The two figures in this appendix show a sample implementation of the WBMGRID programs. Figure 1 is a sample inputs file that runs all four programs, and Figure 2 is a sample Unix script.

```
-----------------------------------------
-----  General Inputs - All Programs   -----
-----------------------------------------
Inputs_File_Built = 03 June 1996 / 12:30:22 GMT
----  Run Control Information  ----
Run_llgrid = 0
Run_geomgrid = 0
Run_irrgrid = 1
Run_s4grid = 0
----  Diagnostic Print Control  ----
IO_DiagPrtFlag = 0
Proc_DiagPrtFlag = 0
----  Files Information  ----
Grid_File = grid_def.bin
Geometry_File = geom_def.bin
EqGeometry_File = eqgeom_def.bin
Irregularity_File = irrgrid.bin
S4_File = s4grid.bin
-------------------------------------
----  Inputs for program llgrid  ----
-------------------------------------
----  Satellite Information  ----
Satellite_Latitude = 0.0
Satellite_Longitude = 275.0
Satellite_Altitude = 36000.0
Satellite_Velocity = 0.0 3000.0 0.0
----  Grid Definition Parameters  ----
Latitude_Spacing = 1.0
Longitude_Spacing = 1.0
Minimum_Elevation = 20.0
Latitude_Limits = -34.0 18.0
Longitude_Limits = 256.0 310.0
--Grid_Def_File = grid_ascii.dat
-------------------------------------
----  Inputs for program geomgrid ----
-------------------------------------
--  There are none!
-------------------------------------
----  Inputs for program irrgrid  ----
-------------------------------------
----  Environment Information  ----
Date = 960320
Time = 0200
F10 = 120.0
Kp = 3.0
Percentile = 90.0
Kp(SS) = 2.0
Kp(SSJ4) = 4.0
----  R/T Data (from analyses)  ----
RT_Longitude_Limits = 260.0 305.0
Analysis_Longitude = 280.0
-- SSIES Analysis Results
SSIES_DateTime = 19960320 013453
SSIES_Kp = 4.0
SSIES_Longitude = 305.0
SSIES_Analysis = 0.75
-- CkL Observations
NonPlume_CkL = 1.32E29
CkL_Observations_Table
960302 1211 -14.35 225.15 1.52E33
960302 1212  15.35 226.15 2.62E33
960302 1213  -2.35 227.15 3.72E33
END_OF_TABLE
----  CkL Latitude Function Output File ----
CkL_Latitude_File = lckl_v_lat.dat
-------------------------------------
----  Inputs for program s4grid  ----
-------------------------------------
Frequency = 250.0
```

Figure 1. Sample WBMGRID system inputs file.

```
#=============================================================================
#  Script for running WBMGRID programs.
#  [Set up to run as a csh script]
#  01 June 1996
#=============================================================================
#  Copyright 1996, Northwest Research Associates, Inc.
#=============================================================================
#
#   Set the name of the inputs file to process.
#
if({$#argv} == 0)then
   set INPUTFILE = testinputs.dat
else
   set INPUTFILE = $argv[1]
endif
#
#   Make sure that the inputs file exists.
#
if(!(-e $INPUTFILE))then
   echo '================================================'
   echo 'ERROR: Inputs file does not exist'
   echo '       File name requested: '$INPUTFILE
   echo '================================================'
   exit
endif
#
#   Set the name of the directory (full path) in which the various
#   executables reside.
#
set BINDIR = /home/salsa/jim/afpl0067/grids/bin
#
#   List out the inputs file.
#
echo '================================================================='
echo 'Listing of inputs file : '$INPUTFILE
cat $INPUTFILE
echo '================================================================='
#
#   Loop over the programs.
#
foreach program ( llgrid geomgrid irrgrid s4grid )
#
   echo STATUS:  Run program $program
   $BINDIR/$program -f $INPUTFILE
   set progstat = $status
   if($progstat != 0)then
      echo '================================================'
      echo 'WARNING:  Bad return status from program '$program
      echo '          Status returned: '$progstat
      echo '================================================'
      break
   endif
   echo '-----------------------------------------------------------------'
#
end
#=============================================================================
```

Figure 2. Sample Unix script for running the WBMGRID programs.

Appendix B. Format of Binary Grid Files

The tables in this appendix show the format and contents of the five grid files used by the WBMGRID programs: Table 1 describes the output grid-definition file from program LLGRID, Table 2 the output geometry file from program GEOMGRID, Table 3 the output equatorial-geometry file from program GEOMGRID, Table 4 the irregularity-parameters output file from program IRRGRID, and Table 5 the S_4 output file from program S4GRID.

Record #1: Header		
Words	Name	Contents
1-5	fileid	Validator string (LLGridDefinitionFile)
6	iymd	YYMMDD file was built
7	ihms	HHMMSS file was built
8	nbout	Number of I/O buffers in file (sans header)
9	nrout	Total number of grid-point records in file
10	nlats	Number of latitudes in grid
11	glat0	Initial grid latitude (rad)
12	dlat	Latitude spacing (rad)
13	nlons	Number of longitudes in grid
14	glon0	Initial grid longitude (rad)
15	dlon	Longitude spacing (rad)
16	el_min	Minimum elevation angle (rad)
17	gca_max	Corresponding maximum GCA (rad)
18	glat_lim(1)	User-input south latitude boundary (rad)
19	glat_lim(2)	User-input north latitude boundary (rad)
20	glon_lim(1)	User-input east longitude boundary (rad)
21	glon_lim(2)	User-input west longitude boundary (rad)
22	slat	Satellite latitude (rad)
23	slon	Satellite longitude (rad)
24	shgt	Satellite altitude (m)
25	vssg(1)	Satellite velocity [+N] (m/s)
26	vssg(2)	Satellite velocity [+E] (m/s)
27	vssg(3)	Satellite velocity [+D] (m/s)
Record #2: Grid-point I/O Record #1		
Words	Name	Contents
1	lbuf	Number of grid-point records in this buffer
2-8		Grid-point record #1
	glat	Grid-point latitude (rad)
	glon	Grid-point longitude (rad)
	ghgt	Grid-point altitude (m)
	az	Ground-to-satellite azimuth (rad)
	el	Ground-to-satellite elevation (rad)
	xlat	Latitude grid index
	xlon	Longitude grid index
9-15		Grid-point record #2
...	...	...
695-701		Grid-point record #100
Record #3: Grid-point I/O Record #2		
...		
Record #N: Grid-point I/O Record #N-1		

Table 1. Contents and format of file `grid.bin`.

Record #1: Header		
Words	Name	Contents
1-5	fileid	Validator string (MainGeometryFile)
6	iymd	YYMMDD file was built
7	ihms	HHMMSS file was built
8	nbout	Number of I/O buffers in file (sans header)
9	nrout	Total number of grid-point records in file
Record #2: Grid-point I/O Record #1		
Words	Name	Contents
1	lbuf	Number of grid-point records in this buffer
2-21		Grid-point record #1
	rlat	Grid-point latitude (rad)
	rlon	Grid-point longitude (rad)
	az	Ground-to-satellite azimuth (rad)
	el	Ground-to-satellite elevation (rad)
	glatp	IPP latitude (rad)
	glonp	IPP longitude (rad)
	hp	IPP altitude (m)
	vspg(1)	Satellite velocity at IPP [+N] (m/s)
	vspg(2)	Satellite velocity at IPP [+E] (m/s)
	vspg(3)	Satellite velocity at IPP [+D] (m/s)
	apxlat	IPP apex latitude (rad)
	apxlon	IPP apex longitude (rad)
	zr	Reduced propagation range (m)
	dec	Magnetic declination at IPP (rad)
	phi	Magnetic ray heading at IPP (rad)
	psi	Magnetic dip at IPP (rad)
	babs	ABS(magnetic field strength) at IPP (gauss)
	theta	Ray elevation angle at IPP (rad)
	nbufe	I/O buffer record for equatorial info
	irece	I/O buffer record index for equatorial info
22-41		Grid-point record #2
...	...	...
1982-2001		Grid-point record #100
Record #3: Grid-point I/O Record #2		
...		
Record #N: Grid-point I/O Record #N-1		

Table 2. Contents and format of file `geom.bin`.

Record #1: Header		
Words	Name	Contents
1-5	fileid	Validator string (EquatorialGeometryFile)
6	iymd	YYMMDD file was built
7	ihms	HHMMSS file was built
8	nbout	Number of I/O buffers in file (sans header)
9	nrout	Total number of grid-point records in file
Record #2: Grid-point I/O Record #1		
Words	Name	Contents
1	lbuf	Number of grid-point records in this buffer
2-17		Grid-point record #1
	glat_pp_base	Latitude of plume base PP (rad)
	glon_pp_base	Longitude of plume base PP (rad)
	erlat_base(1)	Latitude of N E-region base point (rad)
	erlat_base(2)	Latitude of S E-region base point (rad)
	erlon_base(1)	Longitude of N E-region base point (rad)
	erlon_base(2)	Longitude of S E-region base point (rad)
	decapx_base	Magnetic declination at base PP (rad)
	cglat_base	COS(latitude) of base apex (rad)
	glat_pp_top	Latitude of plume top PP (rad)
	glon_pp_top	Longitude of plume top PP (rad)
	erlat_top(1)	Latitude of N E-region top point (rad)
	erlat_top(2)	Latitude of S E-region top point (rad)
	erlon_top(1)	Longitude of N E-region top point (rad)
	erlon_top(2)	Longitude of S E-region top point (rad)
	decapx_top	Magnetic declination at top PP (rad)
	cglat_top	COS(latitude) of top apex (rad)
18-33		Grid-point record #2
...	...	...
1586-1601		Grid-point record #100
Record #3: Grid-point I/O Record #2		
...		
Record #N: Grid-point I/O Record #N-1		

Table 3. Contents and format of file `eqgeom.bin`.

Record #1: Header		
Words	Name	Contents
1-5	fileid	Validator string (IrregularityFile)
6	iymd	YYMMDD file was built
7	ihms	HHMMSS file was built
8	nbout	Number of I/O buffers in file (sans header)
9	nrout	Total number of grid-point records in file
Record #2: Grid-point I/O Record #1		
Words	Name	Contents
1	lbuf	Number of grid-point records in this buffer
2-11		Grid-point record #1
	a	Along-field axial ratio
	b	Cross-field (L-shell) axial ratio
	delta	Sheet/L-shell normal angle (rad)
	alpha	Outer scale-size (rad/m)
	q	In-situ spectral slope
	ckl	Height-integrated spectral strength ($C_k L$)
	rtsw	Real-time section flag (1: R/T section)
	vdpg(1)	In-situ drift velocity at IPP [+N] (m/s)
	vdpg(2)	In-situ drift velocity at IPP [+E] (m/s)
	vdpg(3)	In-situ drift velocity at IPP [+D] (m/s)
12-21		Grid-point record #2
...	...	...
992-1001		Grid-point record #100
Record #3: Grid-point I/O Record #2		
...		
Record #N: Grid-point I/O Record #N-1		

Table 4. Contents and format of file `irrgrid.bin`.

Record #1: Header		
Words	Name	Contents
1-5	fileid	Validator string (S4File)
6	iymd	YYMMDD file was built
7	ihms	HHMMSS file was built
8	nbout	Number of I/O buffers in file (sans header)
9	nrout	Total number of grid-point records in file
Record #2: Grid-point I/O Record #1		
Words	Name	Contents
1	lbuf	Number of grid-point records in this buffer
2-3		Grid-point record #1
	s4	S_4
	rtsw	Real-time section flag (1: R/T section)
4-5		Grid-point record #2
...	...	...
200-201		Grid-point record #100
Record #3: Grid-point I/O Record #2		
...		
Record #N: Grid-point I/O Record #N-1		

Table 5. Contents and format of file `s4grid.bin`.

Appendix C. Longitude Extrapolation of SSIES Analyses

Extrapolating the results of the SSIES analysis in longitude is complicated by the fact that conditions affecting the possible generation of plume structures vary with longitude. Thus, while an SSIES analysis at one longitude might indicate that conditions are good for plume generation, this might not be the case at longitudes not too far removed from the observation longitude due to significant changes in factors that affect plume growth. In particular, the longitude variation of the seasonal modulation of plume generation in WBMOD is based on a hypothesis put forward in *Tsunoda* [1985] that plume generation will be most likely at those times of year when the sunset terminator is aligned with the local geomagnetic meridian. In addition, recent modeling work (such as in *Maruyama* [1988] and *Kelley and Maruyama* [1992]) suggest that the component meridional neutral winds along the geomagnetic meridian can have a "braking" effect on the growth of plumes. This will also vary in some way with the local geomagnetic declination angle near the equator. Given this, we have decided to permit only limited extrapolation of SSIES analyses in longitude sectors where the geomagnetic declination angle varies significantly with longitude and between sectors, and to permit unlimited extrapolation in sectors where the declination is fairly constant in longitude.

Figure 3 illustrates this point and shows the division of the equatorial region into six longitude sectors. Unlimited extrapolation is permitted in sectors 1, 3, and 5; extrapolation is permitted by up to 15° in longitude in sectors 2, 4, and 6; and extrapolation of up to 5° in longitude is permitted from one sector to the next.

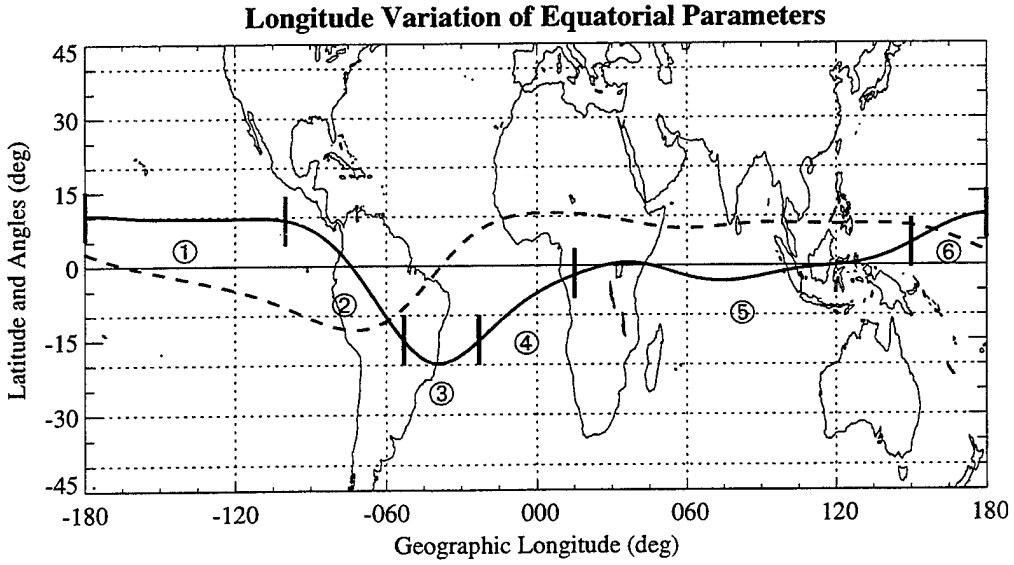

Figure 3. Longitude variation of the apex (dip) equator (dashed line) and the magnetic declination at the equator (solid line). The heavy vertical lines indicate boundaries between the six longitude sectors used in the SSIES analysis.